A guide to hunting periodic three-body orbits with non-vanishing angular momentum☆

Marija R. Janković [a], V. Dmitrašinović [b,*], Milovan Šuvakov [b,c]

[a] *Department of Physics, Imperial College London, 1010 Blackett Lab., Prince Consort Rd., London SW7 2AZ, UK*
[b] *Institute of Physics Belgrade, Belgrade University, Pregrevica 118, Zemun, P.O. Box 57, 11080 Beograd, Serbia*
[c] *Department of Health Sciences Research, Mayo Clinic, 200 First Street SW, Rochester, MN 55905, USA*[1]

ARTICLE INFO

ABSTRACT

A large number of periodic three-body orbits with vanishing angular momentum have been found in Newtonian gravity over the past 6 years due to a simple search method and to the contribution from practitioners outside the Celestial Mechanics community. Extension of such orbits to non-vanishing angular momentum has been lacking due to *inter alia* the absence of a sufficiently simple and widely known search method. We present a method, i.e., a general strategy plus detailed tactics (but not a specific algorithm, or a code), to numerically search for relative periodic orbits in the Newtonian three-body problem with three equal masses and non-vanishing angular momentum. We illustrate the method with an application to a specific, so-called Broucke–Hadjidemetriou–Hénon (BHH) family of periodic 3-body orbits: Our search yielded around 100 new "satellite" orbits, related to the original BHH orbits by a topological relation (defined in the text), with infinitely many orbits remaining to be discovered. We used the so-obtained orbits to test the period vs. topology relation that had previously been established, within a certain numerical accuracy, for orbits with vanishing angular momentum. Our method can be readily: (1) applied to families of periodic 3-body orbits other than the BHH one; (2) implemented using various standard algorithms for solving ordinary differential equations, such as the Bulirsch–Stoer and the Runge–Kutta–Fehlberg ones; (3) adapted to 3-body systems with distinct masses and/or coupling constants, including, but not limited to, Coulomb interaction. Our goal is to enable numerical searches for new orbits in as many families of orbits as possible, and thus to allow searches for other empirical relations, such as the aforementioned topology vs. period one.

© 2019 Elsevier B.V. All rights reserved.

1. Introduction

The three-body problem, as formulated by Newton, is to predict the motion of the Sun–Earth–Moon system [1–5]. Euler [6] and Lagrange [7] found their respective (analytic) solutions in the mid- to late 18th century, but that was of no immediate astronomical significance — the first Jovian satellites were only discovered 150 years after Lagrange's calculation, and even today such Lagrangian systems comprise less than 1% of all known three-body systems, the remaining 99% being the so-called "hierarchical" systems, such as the Sun–Earth–Moon one, [5,8].[2]

In the late 19th century Bruns showed that the general Newtonian three-body problem is not integrable [1], which explained the absence of new solutions at that time. That (should have) made it clear that there would be no further progress without numerical investigations. The first new periodic orbit in the unrestricted three-body problem arrived in 1956 when Schubart [9] found his collinear, and colliding periodic orbit using a mechanical computer.[3]

The numerical studies of periodic orbits in the general, i.e., unrestricted three-body problem (3BP) began in earnest about 50 years ago: The first new orbits after Schubart's one were announced in 1967 by Szebehely and Peters [13,14] who found several "free-fall" periodic orbits using electronic computers.

☆ The review of this paper was arranged by Prof. Hazel Andrew.
* Corresponding author.
  E-mail address: dmitrasin@ipb.ac.rs (V. Dmitrašinović).
[1] On sabbatical leave of absence.
[2] What is meant by "hierarchical" 3-body system is one in which two bodies move around each other, and thus form a "binary", and the third moves around the binary, or *vice versa*.

[3] At about the same time in mid-20th century, doubts about the existence of any further solution, i.e., other than the Eulerian and Lagrangian ones, were formally cast [10], and then equally formally refuted: Arenstorf [11] published an existence proof for periodic solutions of the general three-body problem, albeit without examples, and Jefferys and Moser [12] had also published existence proofs for "almost periodic solutions" in the three-dimensional case, also without examples. Without at least one explicit example of a new periodic orbit, that would have been just another academic controversy.

Subsequently, Standish [15] published several other free-fall orbits. While these publications definitely settled the question of whether the general problem had non-trivial periodic solutions other than the Euler and Lagrange ones, they did not begin to address the question of hierarchical orbits. Moreover, Szebehely and Peters [13,14] suggested that the periodic orbits were isolated.[4] This led to some confusion, which was resolved in 1974 by Hénon [16], who extended Szebehely and Peters' free-fall, i.e., zero-angular-momentum solutions to non-zero values of angular momentum, and showed that they form one-parameter continuous families of orbits. This is a general property of (relative)[5] periodic orbits and will be called Hénon's first theorem.

Further progress was based on this fact and the subsequent numerical discoveries of hierarchical periodic three-body orbits by Broucke's [17,18], Hadjidemetriou's [19–21], and by Hénon's [22–24] groups, working separately, though aware of each other's work, and using different methods. We shall refer to these three groups of authors collectively as BHH. BHH had not only confirmed the existence, but found two kinds ("prograde" and "retrograde", the latter with three branches) of stable periodic solutions, both for equal and unequal masses, as well as for different values of the angular momentum. The stable solutions among those found by BHH are in agreement with observed hierarchical systems [8,17,19]. As the scale-invariant angular momentum[6] is reduced, the hierarchical nature of these solutions is lost, and all three bodies become equally involved in the motion (which is sometimes called "interplay" of three bodies). Such orbits have not been observed, as yet, even though some of them are (linearly) stable. This "lost branch" of BHH solutions remains a challenge for both observational and theoretical astronomy. In the meantime, rigorous existence proofs, at least at certain discrete values of the angular momentum, have been supplied for some of the BHH orbits [26,27]. All of this ought to make it clear that the BHH family of solutions is important, both for astronomical applications and for mathematical purposes, more about which later.

In the meantime, more than 2000 new topologically distinct zero-angular-momentum three-body orbits have been reported [28–43]. By virtue of Hénon's first theorem, each and every one of these orbits defines (the beginning of) a distinct family of orbits with non-zero angular momentum, only a few of which have been studied [30,44–48] to any extent. Though it is practically impossible, at least for one group of investigators, to study all 2000 families, around 45 linearly stable orbits deserve to be further looked into. For such an endeavor, one needs a general method that has been lacking heretofore: the papers [44–47] rely on different techniques designed specifically for one, or another, particular family of orbits. A few years ago we extended a previously established search method for zero-angular-momentum orbits (see Refs. [33,34,37]) to the BHH family of orbits with non-zero angular momentum [39]. It must be emphasized that this search method differs significantly from all three original BHH methods. Indeed, the three BHH methods were designed such that only one (what we now call the progenitor) orbit (at given energy and angular momentum) in the BHH family could be found — the first (and only) satellite orbit (a related orbit, defined in Section 2) of the BHH family, prior to [39], was discovered and reported in Ref. [44], perhaps unwittingly.

As there was no known reason why the number of such satellite orbits ought to be limited – indeed the Birkhoff–Lewis theorem [49] decrees the opposite – the search for BHH satellite orbits had to be conducted, for both practical astronomical and for theoretical reasons. We found around 100 such new orbits, [39], with (infinitely) many more waiting to be discovered, limited only by one's strength and/or patience and availability of computer resources. A similar situation may hold in other families of orbits.

In the meantime, we have realized that our method is sufficiently wide to accommodate searches for periodic orbits in some other, though not all (see Section 3.2), families of the Newtonian gravitational three-body problem, with minimal modifications also for distinct masses; but also in other non-relativistic three-body problem involving homogeneous potentials, such as the Coulombic one [50]. Therefore, the purpose of this work is two-fold:

- methodological: we have extended our previous search and scanning method [34] to periodic orbits with non-zero angular momentum. This was a non-trivial endeavor because one new continuous parameter (angular momentum L) enters the calculation, and the search is necessarily in a three-dimensional subspace of the full six-dimensional phase space of initial conditions, but one with a successful outcome.
  We have modified the method of minimizing the return proximity function in the phase space of initial conditions to the present search in two-dimensional "slices" of a three-dimensional sub-space. This, of course, has the consequence that a detailed search of the complete subspace would last too long to be practically implemented in a reasonably short time. Consequently, we searched only in the immediate vicinity of (previously discovered) progenitor BHH orbits, and, even with this limitation, we found around 100 new orbits.
- particular: to find as many as possible new satellite orbits of the BHH family and then to investigate (any, new) topological regularities among them, such as those discovered among orbits with vanishing angular momentum [36,37]. Davoust and Broucke [44] had found the first (k=3) satellite orbit in the retrograde branch of the BHH family. We extended the search for BHH satellite orbits systematically, at first up to values $k \leq 19$, where k is the so-called topological exponent, defined in Section 2.1 and Ref. [32], and then less systematically up to $k = 84$.[7]

The completion of the long-term goal of exploring the stable families of three-body orbits, as described above, can only be accomplished by a concerted effort by several teams using ever-more-powerful computing facilities. For this reason, here we publish technical details of our search method in the hope that someone else will take over the torch.

This paper is organized into six sections: After the present Introduction, we present necessary preliminaries in Section 2. In Section 3 we discuss our search method and, in particular the subspace of initial conditions. In Section 4 we present our numerical

---

[4] "Recent numerical investigations [13–15] have led to the conjecture that periodic solutions of the planar general problem of three bodies are isolated, for given masses of the bodies. To quote, for instance, Szebehely (1973): 'The periodic orbits of the general problem do not seem to form families in the same sense we know families in the restricted problems'; and 'to establish families of periodic orbits according to what is known today, requires changes in the participating masses as well as in the initial conditions'. This conjecture is made for arbitrary distances between the participating bodies"., a quote from [16].

[5] What is meant here by a relative periodic orbit is one that returns to its initial position after a period, though rotated by a finite angle, see Section 3.1.

[6] The change of angular momentum, while keeping the same form of the orbits, generally implies a change of energy, or of size. Due to the scaling rules [25] for orbits in the Newtonian potential, one can define scale-invariant angular momentum, see Section 2.3.

[7] This is not to say that this sequence stops at 84, but rather, that we have arrived close to the limits imposed by the precision of our codes (and algorithms) and the computing power available to us.

results together with our estimates of numerical uncertainties. Then in Section 5 we discuss the scaling laws for three body orbits and the expected topological dependence of the scaling-law "constant" for three bodies. In Section 6 we discuss the open questions and suggest future searches. Finally, in Section 7 we summarize and draw our conclusions.

2. Preliminaries

In this section we provide some preliminary information, such as the motivation for this work, as well as basic background information necessary to follow the rest of the paper. There is nothing fundamentally new in this section, though it should give a brief pedagogical introduction to matter written for readers unfamiliar with celestial mechanics in general, and the three-body problem in particular.

2.1. Testing new topological laws

Historically, periodic three-body orbits were classified into families and named according to Strömgren's nomenclature used in the restricted three-body problem, see Ref. [44]. Such a definition of families does not always correspond with the unambiguous topological definition of families, provided by Montgomery [51]: For example out of approximately 20 families discussed by Davoust & Broucke [44], only 3 are topologically distinct.

Using the topological classification method, Ref. [33] gave a precise definition of "satellites" of an arbitrary progenitor orbit w, as orbits that are the kth-power of their progenitor, i.e., with the homotopy/free-group elements that have the form w^k, where $k = 2, 3, \ldots$. Thereupon this definition was applied to the study of figure-8 satellites, which were first observed in Ref. [30], and investigated in detail in Ref. [33]. The latter study led to the discovery of remarkable topological Kepler's third law-like regularities ("laws") for orbits with vanishing angular momentum, Refs. [36,37]. An immediate question is if such regularities persist when the angular momentum does not vanish?

Ref. [39] was the first step in an attempt to answer that question, *viz.* that of finding the satellite orbits in the BHH family, as there was no guarantee that they had to exist. The present paper is an elaboration of the brief first report [39]. Indeed, it was only in Ref. [37] that the existence of satellite orbits is related to the stability of progenitor orbit (with vanishing angular momentum) was understood,[8] in terms of the Birkhoff–Lewis theorem [49].

2.2. Basic facts

Broucke [17,18,44], Hadjidemetriou [19–21] and Hénon [22,23] (BHH) explored a set of periodic planar three-body orbits with bodies that have the same mass and wherein the initial coordinates form a collinear configuration (or a "syzygy", as it is known in the astronomical literature),[9]

$$\mathbf{r_1} = (x_1, 0), \mathbf{r_2} = (x_2, 0), \mathbf{r_3} = (x_3, 0)$$

and the initial velocities are orthogonal to the vector determined by the collinear position vectors, i.e., of the form:

$$\mathbf{v_1} = (0, \dot{y_1}), \mathbf{v_2} = (0, \dot{y_2}), \mathbf{v_3} = (0, \dot{y_3})$$

In the following we shall call this a collinear orthogonal configuration. Such configurations are special insofar as they lead

to discrete symmetries of the orbit, when they appear in an orbit twice [53,54]. This is not the most general Ansatz for initial velocities: collinear, i.e., x-components, of relative velocities $\mathbf{v}_i$, $i = 1, 2, 3$, need not vanish in general, but allowing for that freedom would increase the dimensionality of the search phase space by two and thus greatly increase the difficulty of search.

These orbits, an example of which is shown in Fig. 1(a), form two continuous curves of relative periodic orbits in the phase space of initial conditions, whose termini ("ends") include a collinear collision (Schubart) orbit (retrograde), and both approach the limit of a two-body problem with masses m and $2m$ at the common upper terminus ("end") of their $L(T)$ curves, Fig. 2. Concerning the latter limit, the first periodic orbits that Broucke found contained the so-called double Keplerian motion, which means that two bodies revolve tightly around each other, while the pair together revolves around the third body, therefore representing the inner and the outer binary system. If the two binaries' revolve in the same direction, e.g. (both) clock-wise, then the orbit is called direct. If they revolve in opposite directions, then the orbit is retrograde. Some of these orbits have been proven to exist in a mathematically rigorous manner in Refs. [26,27].

Broucke [17,18], Hadjidemetriou [19–21] and Hénon [22,23] talk of two families[10] of orbits – direct and retrograde – but all of these orbits belong to a single topological family: during one period the orbit completes a single "loop" around one of the poles on the shape sphere (for definition see Ref. [32,34]), see Fig. 1.b. This "loop" is described by the conjugacy class of the fundamental group/free group element a, according to the topological classification explained in Refs. [32,34]. It turns out, however, that there are numerous relative periodic orbits with topology a^k, where $k = 2, 3..$, that have the same form of initial conditions. Such orbits are (sometimes) called "satellites" [30,33], whereas other authors call them "bifurcation orbits" [44].

2.3. Scaling laws for Newtonian trajectories

For the sake of clarity and completeness, here we review some elementary scaling laws, indeed so elementary that they are explicitly presented in only one graduate-school level textbook on classical mechanics Ref. [25] that we know of. Nevertheless, these scaling rules have significant non-trivial consequences in the three-body problem. Here we follow our own presentation(s) from Refs. [36,39].

It is well known that Kepler's third law follows from the spatio-temporal (mechanical) scaling laws, which, in turn, follow from the homogeneity of the Newtonian gravity's potential. Under spatial scaling $\mathbf{r} \rightarrow \lambda\mathbf{r}$, the time must scale as $t \rightarrow \lambda^{3/2}t$, and consequently $\mathbf{v} \rightarrow \mathbf{v}/\sqrt{\lambda}$. The (total) energy scales as $E \rightarrow \lambda^{-1}E$, the period T as $T \rightarrow \lambda^{3/2}T$ and the angular momentum as $L \rightarrow \lambda^{1/2}L$, the last one behaving differently than either the period T, or the hyper-radius $R = \sqrt{\frac{1}{3}\sum_{i<j}^3(\mathbf{r}_i - \mathbf{r}_j)^2} = \sqrt{\sum_i^3(\mathbf{R}_{\mathrm{g.b.}} - \mathbf{r}_i)^2}$, which is proportional to the root-mean-square distance of the three particles from their geometrical barycenter $\mathbf{R}_{\mathrm{g.b.}} = \frac{1}{3}\sum_i^3 \mathbf{r}_i$,[11] and scales linearly with λ: $R \rightarrow \lambda R$ thus presenting a measure of the overall "size" of the triangle. The angular momentum L, though conserved by virtue of the equations of motion, changes ("scales") as a function of the total energy E, or of the "size" R. For this reason only vanishing angular momentum

---

[8] In Ref. [39] the (unnecessarily strong) KAM theorem was invoked when the (weaker) Birkhoff–Lewis one would have sufficed.

[9] Which is in conformity with Montgomery's theorem, [52], that, with the exception of Lagrange's solution, every periodic solution to the Newtonian three-body problem passes through syzygies.

[10] whereas Davoust and Broucke [44] relate further three families (D_2, D_3, D_4) to the BHH family D_1 by way of analytic continuation through binary collisions; see "... although it is very likely that the four families D_1 through D_4 are, in fact, one single complex family" in Sect. 7. of Ref. [44].

[11] which equals the physical center-of-mass $\mathbf{R}_{\mathrm{g.b.}} = \mathbf{R}_{CM}$ when all three masses are equal.
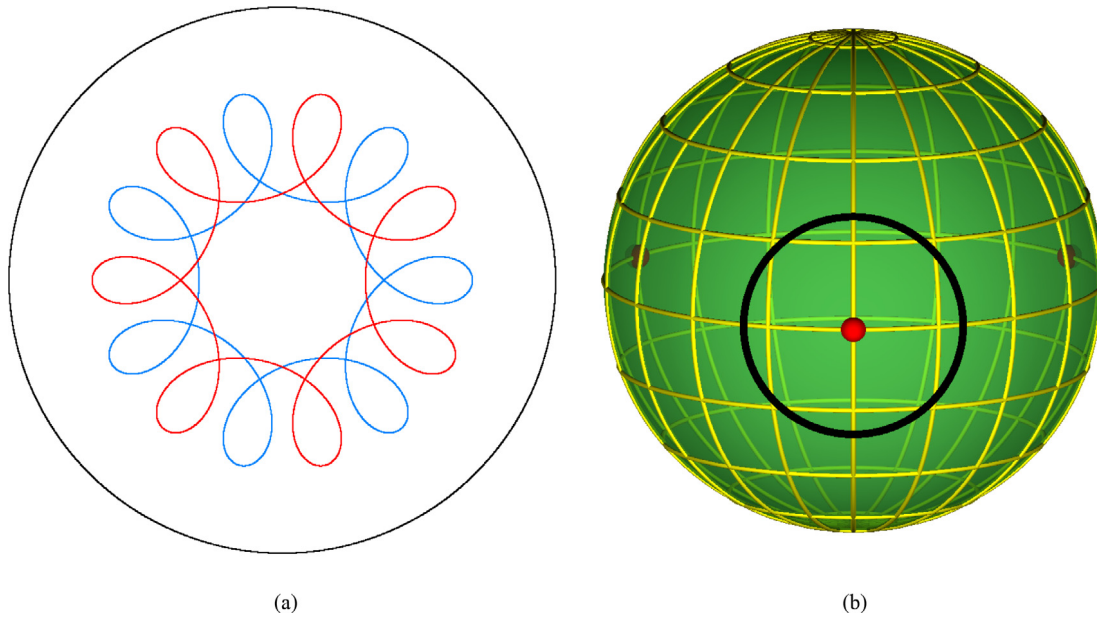
Fig. 1. (a) One retrograde BHH orbit, an absolute periodic one. It can be obtained from a particular relative periodic orbit whose period is multiplied by 7, after which time the orbit closes its trajectory in real space. (b) the same orbit on the shape sphere.
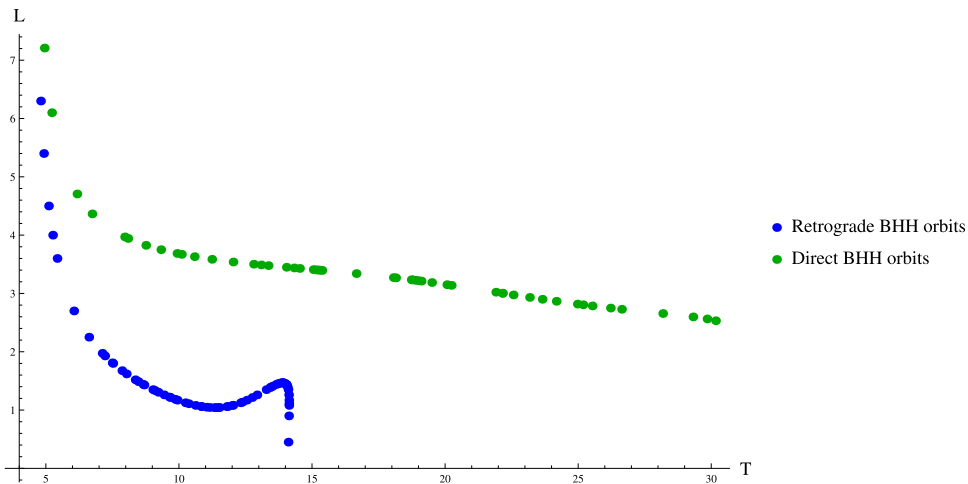
Fig. 2. $L(T)$ curves for (a) direct (prograde) orbits (green dots); and (b) retrograde BHH orbits (blue dots). All orbits are scaled to have total energy $E = -\frac{1}{2}$. Figure reproduced from Ref. [39] with permission from the publisher. (For interpretation of the references to color in this figure legend, the reader is referred to the web version of this article.)

$L = 0$ is a "fixed point" under scaling transformations. Therefore, in the following we shall use the scale-invariant angular momentum $L_r = L|E|^{1/2}$[12] and, for simplicity's sake, equal masses. Thus, we (may) replace the (typical, or mean, or maximum) "size" $\bar{R}$ of the three-body system in Kepler's third law $T \propto \bar{R}^{3/2}$ with the inverse absolute value of energy $|E|^{-1}$, i.e., $T \propto |E|^{-3/2}$, or equivalently $T|E|^{3/2} = $ const. . These scaling laws hold for any number of bodies interacting by Newtonian gravity.

The "constant" on the right-hand-side of the equation $T|E|^{3/2}$ = const. is not universal in the three-body case, as it is in the two-body case — it may depend on all or any one of the following:

the topological family w of the three-body orbit, described by the free-group word w, on the mass ratios, and on the scale-invariant angular momentum $L_r = L|E|^{1/2}$, see Refs. [22,23]

$$T^{(w)}|E|^{3/2} = f(L^{(w)}|E|^{1/2}),$$

or as an inverse function:

$$L^{(w)}|E|^{1/2} = f^{-1}(T^{(w)}|E|^{3/2}).$$

Thus, the curve $L_r^{(w)}(T_r^{(w)}) = L^{(w)}|E|^{1/2}(T^{(w)}|E|^{3/2})$ as a function of $T_r^{(w)} = T^{(w)}|E|^{3/2}$ is a fundamental property of any family w of periodic three-body orbits. For the BHH family the $L(T)$ curve shown in Fig. 2 is based on the data from Refs. [17–23].

---

[12] Davoust and Broucke [44] used the combination of variables $27L^2E$, which is effectively the negative of 27 times the square of L_r.

2.4. The return proximity function

The return proximity function $d(\mathbf{X}_0, T_0)$ in phase space is defined as the absolute minimum of the $d(\mathbf{X}_0, T_0) = \min_{t_m < t \leq T_0} \left| \mathbf{X}(t) - \mathbf{X}(0) \right|$, of the 12-dimensional state vector $\mathbf{X}_0 = \mathbf{X}(t) - \mathbf{X}(0)$ evolving from the initial time 0 to the time t, where

$$\left| \mathbf{X}(t) - \mathbf{X}(0) \right| = \sqrt{\sum_i^3 [\mathbf{r}_i(t) - \mathbf{r}_i(0)]^2 + \sum_i^3 [\mathbf{p}_i(t) - \mathbf{p}_i(0)]^2} \quad (1)$$

is the Euclidean norm ("distance" between two 12-vectors) in the 12-dimensional Euclidean phase space consisting of the Cartesian coordinates and velocities of all three bodies without removing the center-of-mass motion, and t_m is the shortest non-zero time such that $\left. \frac{d \left| \mathbf{X}(t) - \mathbf{X}(0) \right|}{dt} \right|_{t=t_m} = 0$. The recurrence time $\tau(\mathbf{X}_0, T_0)$ is the time t at which a minimum of $\left| \mathbf{X}(t) - \mathbf{X}(0) \right|$ is reached. Searching for periodic solutions with a period $T < T_0$ is equivalent to finding zeros of the return proximity function.

A definition analogous to Eq. (1) holds for the 8-vector $\mathbf{Y}(t)$, made up of Jacobi relative vectors $(\boldsymbol{\rho}, \boldsymbol{\lambda})$:

$$\boldsymbol{\rho} = \frac{1}{\sqrt{2}} (\mathbf{r}_1 - \mathbf{r}_2)$$

$$\boldsymbol{\lambda} = \frac{1}{\sqrt{6}} (\mathbf{r}_1 + \mathbf{r}_2 - 2\mathbf{r}_3)$$

and their time derivatives $(\dot{\boldsymbol{\rho}}, \dot{\boldsymbol{\lambda}})$; here we have eliminated the center-of-mass vector and its corresponding linear momentum from the phase space. Similarly, the 6-vector $\mathbf{Z}(t) = (x, y, z, \dot{x}, \dot{y}, \dot{z})$ consisting of "three-vectors" (x, y, z)

$$x = \frac{2\boldsymbol{\rho} \cdot \boldsymbol{\lambda}}{R^2}, \quad y = \frac{\boldsymbol{\lambda}^2 - \boldsymbol{\rho}^2}{R^2}, \quad z = \frac{2(\boldsymbol{\rho} \times \boldsymbol{\lambda}) \cdot \boldsymbol{e}_z}{R^2} \quad (2)$$

where $R = \sqrt{\boldsymbol{\rho}^2 + \boldsymbol{\lambda}^2}$ is the hyper-radius, which are scalar products of Jacobi vectors, and thus rotation-invariant, and their time derivatives $(\dot{x}, \dot{y}, \dot{z})$.

3. The space of initial conditions for BHH orbits

In the preceding section we showed some of the arguments used by BHH, as well as some of their results. In the following we present our method and describe its advantages.

3.1. Relative periodic orbits

Relative periodic orbits are such that the system returns, after one period, to its initial configuration, albeit rotated through some angle. When this total rotation angle equals zero, or is a multiple of 2π, the solution is called absolute periodic. A relative periodic orbit with a total rotation angle that is commensurate with 2π yields, after a certain number of periods, an absolute periodic orbit. All of the BHH orbits are relative periodic, and some of them also lead to absolute periodic orbits.

Therefore, we shall search only for relative periodic orbits, by eliminating the rotations, i.e., by using the 6-vector, $\mathbf{Z}(t) = (x, y, z, \dot{x}, \dot{y}, \dot{z})$, defined in Eq. (2). The overall (total) rotation angle Φ of the system can be reconstructed from the trajectory in this hyper-space and the equation for angular momentum conservation. By using the relative return proximity function, $d(\mathbf{Z}_0, T_0) = \min_{t_m < t \leq T_0} |\mathbf{Z}(t) - \mathbf{Z}_0|$, in the minimization procedure, Refs. [32,34,39], we are effectively searching for relative periodic orbits.

The collinear orthogonal configuration is a fixed point of a reversing symmetry [17,53,54] and as such has consequences for periodic orbits in the problem of three-bodies, as noted already by Broucke and Boggs [17] and by Bengochea et al. [55]. If an orbit passes through two, or more, collinear orthogonal configurations, then it possesses a higher (discrete) symmetry, as formalized in the "mirror theorem", Refs. [17,53–55]. We shall find multiple examples of such discrete symmetries among our three-body orbits.

3.2. Parametrization of initial conditions

Montgomery [52] has shown that all periodic 3-body orbits, with the exception of the Lagrange one, must encounter a syzygy, or equivalently cross the equator on the shape sphere, at least once during one period. Thus, by choosing a collinear configuration (a syzygy), though not necessarily a collinear orthogonal configuration for the initial one, one does not lose generality. Thus one reduces the number of independent Cartesian components of initial relative vectors and velocities from eight down to six. Therefore, the most general parametrization of initial conditions involves six parameters: (1) two for the initial configuration; and (2) four for the initial velocities. Fixing one of two initial configuration parameters can be thought of as constraining the initial size of the system, which reduces the number of free parameters to five.

The energy and the angular momentum conservation impose two further linearly independent, but non-linearly related constraints on the initial vectors and velocities. Indeed, fixing the energy at a particular value is equivalent to choosing a particular initial size of the system, so we shall leave these intricacies for Section 3.2.2. Five-dimensional search space is still too large for practical implementation. Therefore, we chose to set two collinear components of the initial relative velocities equal to zero, and keep only the orthogonal ones. This choice reduces the number of parameters to three.

The same choice is consistent with, i.e., sufficient but not necessary for, vanishing of the time derivative of the hyperradius R at the initial (syzygy) time $t = 0$: $\dot{R}(t = 0) = 0$, see Section 3.2.2. In other words $\dot{R}(t = 0) = 0$, does not imply orthogonality of the initial velocities to the initial vector. The additional initial constraint $\dot{R}(t = 0) = 0$ is satisfied by all of the (non-zero-angular-momentum) BHH orbits [17–23], and by all of the (non-zero-angular-momentum) Davoust–Broucke orbits [44], as well as by all of the (zero-angular-momentum) solutions in Refs. [33,37,42,43]. Thus, the collinear orthogonal initial configuration is sufficiently wide to encompass many, though not all of presently known families of periodic orbits. One exception is Martin Grant's Rosette orbit, Ref. [56], for his initial conditions see footnote.[13] This set of i.c.s appears to have 8 independent variables. By evolving to a collinear configuration this number is reduced to six, see Section 6.2.4. One of two initial configuration parameters may be fixed (e.g. to unity, as in Section 3.3) which leaves us with five free parameters in total, which is more than the three parameters allowed in our search subspace. This means that this solution does not fit into the class with collinear orthogonal initial conditions. Nevertheless, this orbit passes through 3 "reversor" isosceles configurations, which fact guarantees additional discrete symmetry of the orbit.

---

[13] Martin Grant's i.c.s are: $x_1(0) = 0.7812$, $y_1(0) = -0.2465$, $x_2(0) = y_1(0) = -0.2465$, $y_2(0) = x_1(0) = 0.7812$, $x_3(0) = -x_1(0) - x_2(0) = -0.5347$, $y_3(0) = x_3(0) = -0.5347$, $\dot{x}_1(0) = -\dot{y}_2(0) = -0.6087$, $\dot{y}_1(0) = -\dot{x}_2(0) = -0.286$, $\dot{x}_3(0) = -\dot{x}_1(0) - \dot{x}_2(0) = 0.3227$, $\dot{y}_3(0) = -\dot{x}_3(0) = -0.3227$, $T = 17.0874$, $E = -1.89451$, $L = -0.40184$.
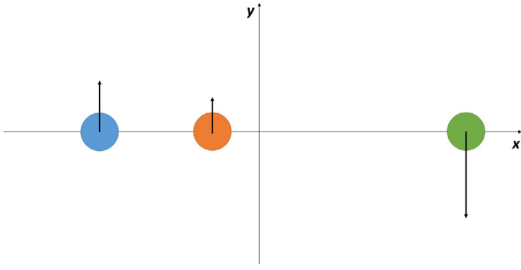
Fig. 3. Geometry of initial conditions.

3.2.1. Initial configuration

The initial configuration is collinear, (or recti-linear) orthogonal, though generally asymmetric, as shown in Fig. 3, so as to yield non-zero angular momentum, and can be written in terms of (initial configuration) Jacobi vectors $\boldsymbol{\rho}_0, \boldsymbol{\lambda}_0$ as:

$$\boldsymbol{\rho}_0 = (a, 0), \quad \boldsymbol{\lambda}_0 = (b, 0),$$

and the initial position of the center-of-mass (CM)

$$\mathbf{R}_0^{\mathrm{CM}} = \frac{1}{3}\left(\mathbf{r}_0^1 + \mathbf{r}_0^2 + \mathbf{r}_0^3\right) = \frac{1}{3}\left(x_1 + x_2 + x_3\right)\hat{\mathbf{x}} = 0$$

From these three linear algebraic equations one can easily find

$$x_3 - x_1 = -\frac{a + \sqrt{3}b}{\sqrt{2}}, \quad x_3 - x_2 = \frac{a - \sqrt{3}b}{\sqrt{2}}, \quad x_1 - x_2 = \sqrt{2}a,$$

(3)

the initial potential energy equals

$$V = -\sum_{i<j}\frac{1}{r_{ij}} = -\left(\frac{\sqrt{2}}{a + \sqrt{3}b} + \frac{\sqrt{2}}{|a - \sqrt{3}b|} + \frac{1}{\sqrt{2}a}\right),$$

(4)

and the initial hyper-radius is $R_0 = \sqrt{\boldsymbol{\rho}_0^2 + \boldsymbol{\lambda}_0^2} = \sqrt{a^2 + b^2}$.

3.2.2. Initial velocities

We demand that the CM velocity vanishes

$$\dot{\mathbf{R}}_{CM} = \frac{1}{3}\left(\dot{\mathbf{r}}_1 + \dot{\mathbf{r}}_2 + \dot{\mathbf{r}}_3\right) = 0$$

which leaves four independent components of two two-dimensional Jacobi velocity vectors, as advertised earlier.

Next, we impose $\dot{R}(0) = 0$ as an initial condition. The hyperradius R can be expressed as $R = \sqrt{\rho^2 + \lambda^2}$, a function of the Jacobi vectors $\boldsymbol{\rho}, \boldsymbol{\lambda}$. This leads to the requirement

$$R(0)\dot{R}(0) = \boldsymbol{\rho}_0 \cdot \dot{\boldsymbol{\rho}}_0 + \boldsymbol{\lambda}_0 \cdot \dot{\boldsymbol{\lambda}}_0 = 0,$$

as $R(0) \neq 0$. Since $(\boldsymbol{\rho}_0, \boldsymbol{\lambda}_0)$ have only components in one (the x-) direction, the above equation imposes a constraint only on a linear combination of the x-components of the velocity vectors, and no condition on the orthogonal (y-) components, which are, in turn, determined by the angular momentum

$$L = m\left(\boldsymbol{\rho}_0 \times \dot{\boldsymbol{\rho}}_0 + \boldsymbol{\lambda}_0 \times \dot{\boldsymbol{\lambda}}_0\right).$$

This is most simply solved by the requirement that the initial velocity vectors have no x-component, i.e., that they are parallel, and orthogonal to the initial spatial separation vectors:

$$\dot{\boldsymbol{\rho}}_0 = c\hat{\mathbf{y}} = \frac{1}{\sqrt{2}}\left(\dot{y}_1 - \dot{y}_2\right)\hat{\mathbf{y}},$$

$$\dot{\boldsymbol{\lambda}}_0 = d\hat{\mathbf{y}} = \frac{1}{\sqrt{6}}\left(\dot{y}_1 + \dot{y}_2 - 2\dot{y}_3\right)\hat{\mathbf{y}},$$

which leaves us with two additional free parameters (c, d).

Of course, this is not the most general set of initial conditions satisfying our additional constraint $\dot{R}(0) = 0$ — it can be augmented/extended by adding two new parameters, the x-components of the velocity vectors, $e = \dot{\rho}_x, f = \dot{\lambda}_x$, that satisfy

$$\rho_x\dot{\rho}_x + \lambda_x\dot{\lambda}_x = 0,$$

thus leaving (only) one independent new parameter.

Our Ansatz $e = f = 0$ is sufficiently wide to cover the BHH family and its topological satellites, as well as other families of orbits (such as, though not limited to, the non-zero-angular-momentum BHH orbits [17–23] and by (some of) three non-zero-angular-momentum Davoust–Broucke orbits [44], and, last but not least, all of the zero-angular-momentum solutions in Refs. [33,37,42,43]).

Thus our space of initial conditions is nominally four-dimensional, with an additional (non-linear) constraint between the angular momentum and energy. The energy E is determined by

$$E = \frac{1}{2}\left(\mathbf{v}_\rho^2 + \mathbf{v}_\lambda^2\right) - \sum_{i<j}\frac{1}{r_{ij}} = \frac{1}{2}\left(c^2 + d^2\right)$$
$$- \left(\frac{\sqrt{2}}{a + \sqrt{3}b} + \frac{\sqrt{2}}{|a - \sqrt{3}b|} + \frac{1}{\sqrt{2}a}\right)$$

(5)

(we take all three masses to equal $m = 1$, and set the gravitational constant $G = 1$, which sets the units in our system). The total angular momentum is given by

$$L = |\boldsymbol{\rho} \times \dot{\boldsymbol{\rho}}| + |\boldsymbol{\lambda} \times \dot{\boldsymbol{\lambda}}| = ac + bd,$$

both of which are constants of motion. As briefly mentioned above, one might think that these two integrals of motion could be used to effectively remove one of the three parameters. The energy is related to the overall size (hyper-radius R) by scaling rules, Section 2.3. So it will be used up when we fix the size see Section 3.3. The angular momentum, on the other hand, scales with size differently than the energy, so that, in effect, it remains an independent variable. Thus, our space of initial conditions of BHH orbits remains effectively three-dimensional, even when these two conservation laws are explicitly implemented.

3.3. The search sub-space

We use these four parameters (a, b, c, d), together with the following additional constraint to parametrize the search-space for periodic orbits. The "size" of the orbits must be fixed in order to avoid finding the same orbits, only rescaled by a size factor, see Section 2.3. Therefore, we fix the "size" by setting $b = 1$. Henceforth we shall not rescale the size R, or energy E of the system.[14]

Then, for any fixed value of L, we have $d = L - ac$, and with energy $E = \frac{1}{2}\left(c^2 + (L - ac)^2\right) - \left(\frac{\sqrt{2}}{a + \sqrt{3}} + \frac{\sqrt{2}}{|a - \sqrt{3}|} + \frac{1}{\sqrt{2}a}\right)$, a function of three independent variables: a, c and L. Now we are left with (only) a three-dimensional "phase sub-space", spanned by a, c and L, to be searched for periodic orbits. For a fixed value of L the search can be further restricted to certain regions of parameters a and c (see the following).

Firstly, as three equal masses imply permutation symmetry, one only needs to look at one permutation of the three bodies, thus allowing us to search only a limited set of configurations *viz.* starting from those in which the "inner body" is closer to the "left-hand-side" body, to the configurations when the "inner

---

[14] Only at the end of the day, one may change to scale-invariant period and angular momentum.
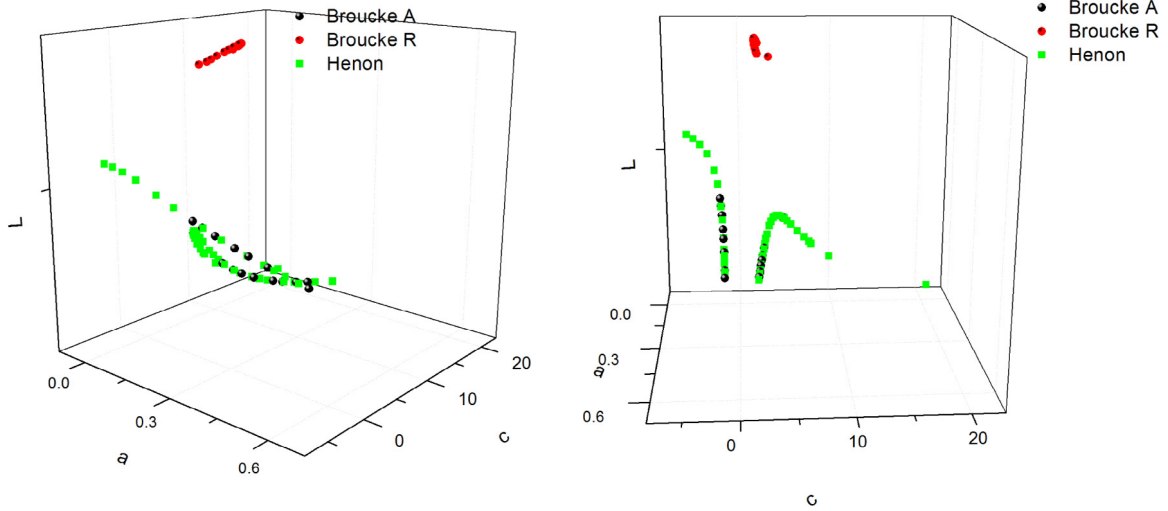
Fig. 4. Two views of the three-dimensional parameter space of the initial conditions of BHH orbits. Green points denote Hénon's (retrograde) orbits [22], black points are Broucke's "A family" (retrograde) orbits and the red points denote Broucke's "R family" (prograde) orbits [18]. (For interpretation of the references to color in this figure legend, the reader is referred to the web version of this article.)

body" is exactly in the middle between the other two bodies, i.e., for $a \in (0, \frac{1}{\sqrt{3}}]$, we have $|a - \sqrt{3}| = \sqrt{3} - a$ and leads to

$$E = \frac{1}{2}\left(c^2 + (L - ac)^2\right) - \frac{1}{\sqrt{2}a} + \frac{2\sqrt{6}}{a^2 - 3}.$$

Secondly, we confine ourselves to the values of free parameters that lead to negative total energies, $E < 0$, so as to avoid escape of one of the bodies to infinity.[15] For example, having fixed the values of L and a, the allowed values of c lie within a circle defined by the inequality:

$$\frac{1}{2}\left(c^2 + (L - ac)^2\right) < \frac{1}{\sqrt{2}a} + \frac{2\sqrt{6}}{3 - a^2}. \tag{6}$$

This inequality has non-trivial implications: it divides the (a, c, L) space into disjoint regions, some of which are allowed, and others are not.

The inequality (6) can be rewritten in various ways, keeping one pair of parameters fixed while solving for the third one; thus it is quartic in a, and quadratic in c, and L. As some of its roots need not be real, or within the allowed regions of (real-valued) parameters the actual number of relevant roots may be anywhere between 0 and $4 \times 2 \times 2 = 16$, which determines the number of allowed, disjoint regions in the (a, c, L) space. E.g. depending on whether e.g. $c \in (c_-, c_+)$, or $c \in (0, c_-)$, $c \in (c_+, \infty)$

$$c_\pm = \frac{aL}{(a^2 + 1)} \mp \frac{1}{(a^2 + 1)}$$
$$\times \sqrt{\frac{\left(a\left((a^2 - 3)L^2 + \sqrt{2}\left(a\left(-a^2 + 4\sqrt{3}a + 2\right) + 4\sqrt{3}\right)\right) + 3\sqrt{2}\right)}{-a(a^2 - 3)}}$$

and, e.g. $L \in (L_-, L_+)$, or $L \in (0, L_-)$, $L \in (L_+, \infty)$, where

$$L_\pm = ac \pm \sqrt{\frac{\left(a\left(a\left(\sqrt{2} - ac^2\right) + 3c^2 - 4\sqrt{6}\right) - 3\sqrt{2}\right)}{a(a^2 - 3)}}$$

It should be clear that the number and form of these restrictions depends on the functional dependence $L(a, c)$ for any given family

of periodic orbits. As these $L(a, c)$ functional dependences are generally not known, except in one (the BHH), or perhaps two cases (the figure-8 orbits), in the following we shall eschew a general analysis of all possible cases, such as the one above, but concentrate on the case of BHH orbits at hand.

Before we continue, a few comments are in order: (1) it should be clear that the present method can be readily modified to include distinct masses; (2) at first we shall apply this method to the BHH family, as that is the most thoroughly studied family of three-body orbits in the literature and the $a(L, c)_{BHH}$ is fairly well known; (3) the present method holds in general, and not only for the BHH family. It can and should be applied in the vicinity of all known (linearly) stable orbits with vanishing angular momentum.

3.4. The region of BHH orbits' initial conditions and the scanning method

As can be seen in Fig. 4 all of the previously known BHH orbits fall on two continuous "curves", the green–black one depicting the retrograde, and the red one the prograde orbits, in the three-dimensional space of initial conditions parametrized by L, a and c.[16] This is a consequence of Hénon's first theorem [16]. Therefore, we choose the vicinity of this structure as the starting point of our search. Our search was conducted at fixed values of angular momentum L, in a region of a two-dimensional subspace of initial conditions parametrized by a and c. The "scanning" method for numerical searching for relative periodic orbits, which is described in more detail in Ref. [34] consists of two steps: (1) a "brute force" scan that produces the "initial candidates"; and (2) use the "initial candidates" as starting points in a minimization method, such as coordinate descent, or gradient descent. The crux of the matter is to have a good idea where to look for candidates, which depends on the parametrization of the initial conditions. The resulting orbit is accepted as periodic if the minimized r.p.f. is sufficiently close to zero.

---

[15] This condition alone does not guarantee that there can never be an escape to infinity, but only that there will be none as long as there are no two-body collisions.

[16] N.B. The retrograde orbits' "one continuous" curve appears as two here due to our choice of the domain of the parameters a and c, and of symmetries; another choice might have given a single curve, which, however, would have been less auspicious for the purposes of orbit hunting. Similarly, the prograde and the retrograde curves would merge in the (extreme) limit of two "inner" bodies merging into one.
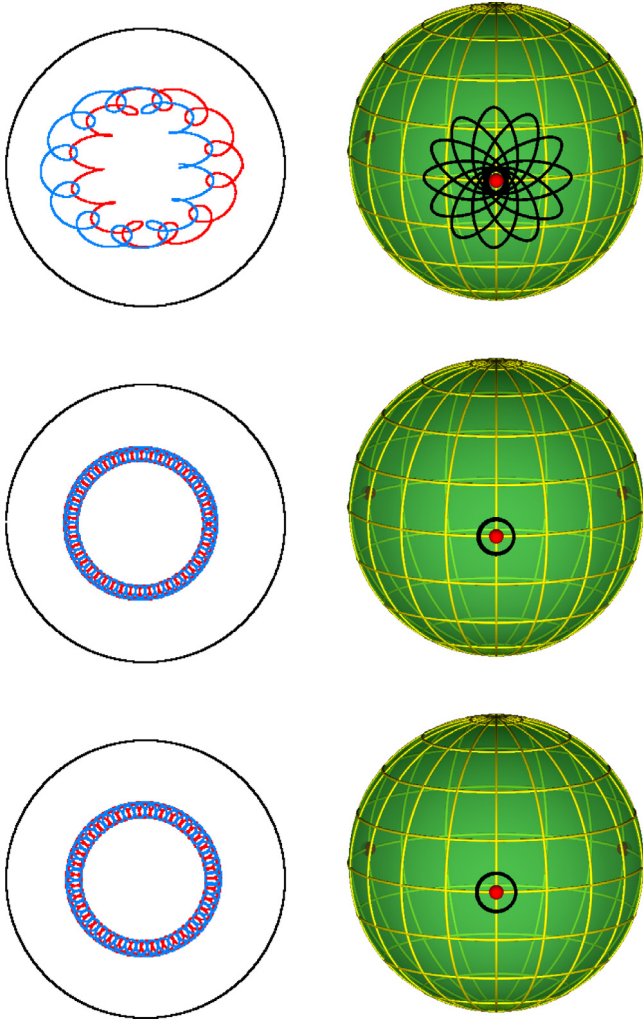
Fig. 5. Initially discovered satellite orbits of the BHH family, shown in real space and on the shape sphere, $k = 12, 45, 39$.
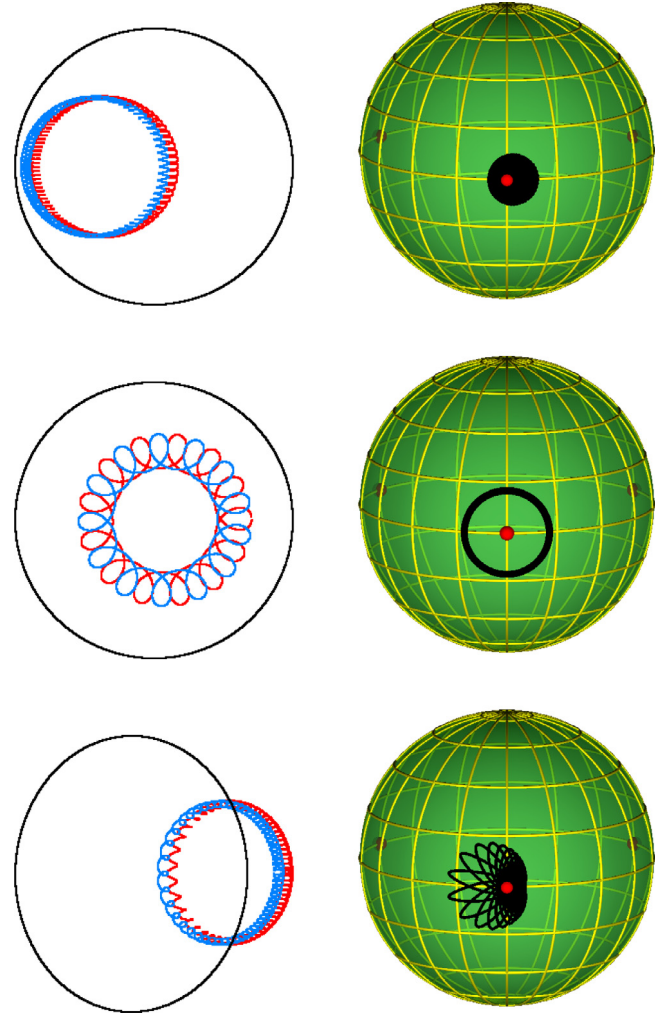
Fig. 6. Initially discovered satellite orbits of the BHH family, shown in real space and on the shape sphere, $k = 84, 13, 58$.

4. Results

Our search was conducted at fixed values of angular momentum L, in a region of a two-dimensional subspace of initial conditions parametrized by a and c. The "scanning" method of numerical searching for periodic orbits was briefly explained in Section 3.4 and described in pedagogic detail in Ref. [34].

We performed two preliminary searches at angular momentum $L = 0.935549$, where there is one (Hénon's) orbit, and at $L = 1.5$, where there are no BHH orbits. Parameters a and c took values in the following intervals: $a \in [0.05, 0.6]$, $c \in [-5.5, 5.5]$, although it was unnecessary to go above $a = 1/\sqrt{3} = 0.57735 \cdots$, see Section 3.3. The resolution of the search was 1000×1000, which determined the duration of search. Naturally, one expects that longer searches would have produced more copious results, as longer periods would have been probed.

Some local minima of the return proximity function (r.p.f.) were extracted from the results and refined using additional minimization methods, which led to several new orbits, some of which were direct, whereas others were retrograde. After plotting the newly found orbits' trajectories on the shape sphere, it was

easy to see that all of these orbits are topological powers of BHH orbits, the so-called topological satellites.

In the first two (preliminary) searches we found six BHH satellite orbits. These orbits make k loops about a single collision point on the shape sphere, with $k = 84, 12, 45, 39, 58, 13$ (see Figs. 5 and 6), some of which are retrograde and others are direct. One notices immediately the diversity of patterns on the shape sphere: some (e.g. panels 2, 3, 4, 6 in Fig. 5) are symmetric, whereas others (e.g. panels 1, 5 in Fig. 5) are asymmetric.

However, the level of detail in these results is very low: the resolution is not high enough to resolve some minima. Therefore we decided to perform such "scans" in smaller sections of the $a-c$ plane and in the vicinity of BHH orbits (see Figs. 7 and 8).

4.1. High resolution searches for BHH satellite orbits

The maps of the return proximity function at $L = 0.8, 0.85, 0.9, 0.935$ are shown in Figs. 7 and 8. Note the "interference-like" dark and bright regions (patterns) in this map. The brighter regions correspond to higher values of the negative logarithm of the return proximity function. Each bright (yellow) "stripe" in Figs. 7, 8 contains a particular satellite of topological order
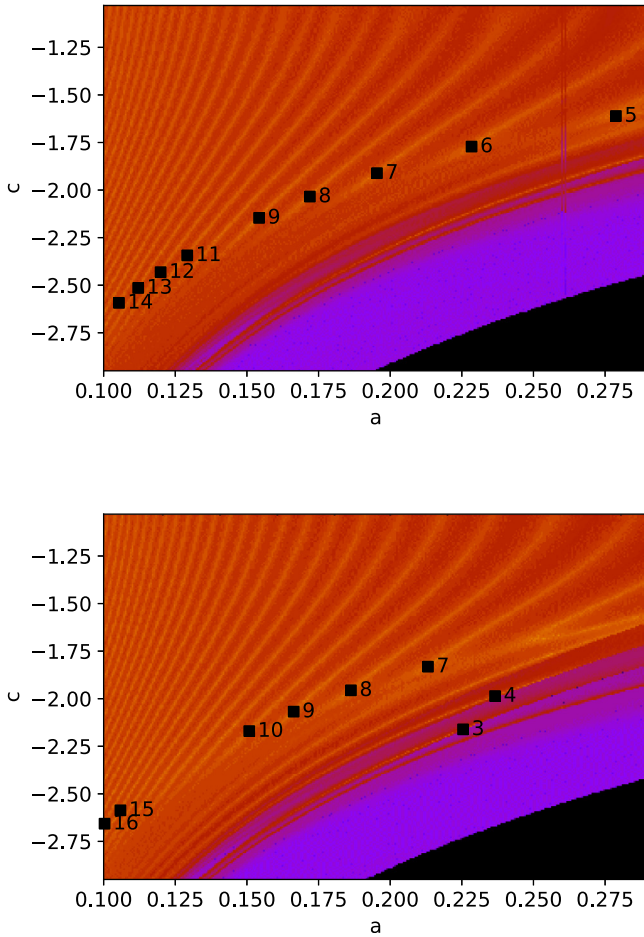
Fig. 7. The map of the negative logarithm of the return proximity function at angular momentum values $L = 0.8$ (upper panel), and $L = 0.85$ (lower panel). The brighter regions correspond to higher values of the negative logarithm of the return proximity function. Each black square denotes a local minimum of the return proximity function for which the value of the return proximity function is sufficiently close to zero: a satellite orbit, and the number is the k-value of that satellite. The black region in the lower right-hand corner is forbidden by the negative energy condition.

Fig. 8. The map of the negative logarithm of the return proximity function at angular momentum values $L = 0.9$ (upper panel), and $L = 0.935549$ (lower panel). The brighter regions correspond to higher values of the negative logarithm of the return proximity function. Each black square denotes a local minimum of the return proximity function for which the value of the return proximity function is sufficiently close to zero: a satellite orbit, and the number is the k-value of that satellite. The black region in the lower right-hand corner is forbidden by the negative energy condition.

k, arranged in an increasing order of k from the right to the left-hand side (see Figs. 10 and 11).

The same region in the $a - c$ plane was also explored at four other values of $L \in [0.8, 1]$. There we found satellite orbits with the same values of k, at slightly different initial conditions. For example, their trajectories on the shape sphere were wider or narrower, and for one of the two visually distinct types in Fig. 12, the satellites of the same k differ in eccentricity.

Some shape-sphere orbits (e.g. panels 1, 2, 3 in Fig. 12) are symmetric, whereas others (e.g. panels 4, 5 in Fig. 12) are asymmetric. In Fig. 12 one can also recognize that there are orbits with significant eccentricities of the inner and outer binaries, where these two kinds of binaries can (still) be recognized. In contrast, we challenge the reader to recognize any kind of binary in the satellite orbits shown in panel 1 of Fig. 12].

All of these satellites at the above-mentioned values of L are "arranged" in a way similar to those at $L = 0.9$, and in an overall manner/shape that are in accordance with Hénon's first theorem, i.e., with the expectation that there are continuous families (curves in the parameter space) of satellite orbits with a particular value of k, and most probably several different families/curves for the same k.

In addition to this, we searched for satellites with higher powers k, at higher values of angular momentum L, where we found examples of k up to 58.

4.2. Detailed searches near BHH retrograde orbits

Summary of detailed searches that were performed in the vicinity of BHH retrograde orbits is given in Table 1, with the searched segments of parameter space illustrated in Fig. 9. Comments made in the right-hand-most column of Table 1 indicate segments open to future improvement. One, particularly interesting segment is the low L-values, which we could not access due to lack of regularization of collisions in our code. Orbits in this region ought to have satellites, as well, assuming relevance of the Birkhoff–Lewis theorem to this system, see Section 6.1. A detailed study of this segment would constitute a test of this assumption.

The complete set of orbits is shown in the text below; the topological power k takes values $k = 3$–48, 58, 84, see Fig. 12. For more, see the web-site [38].
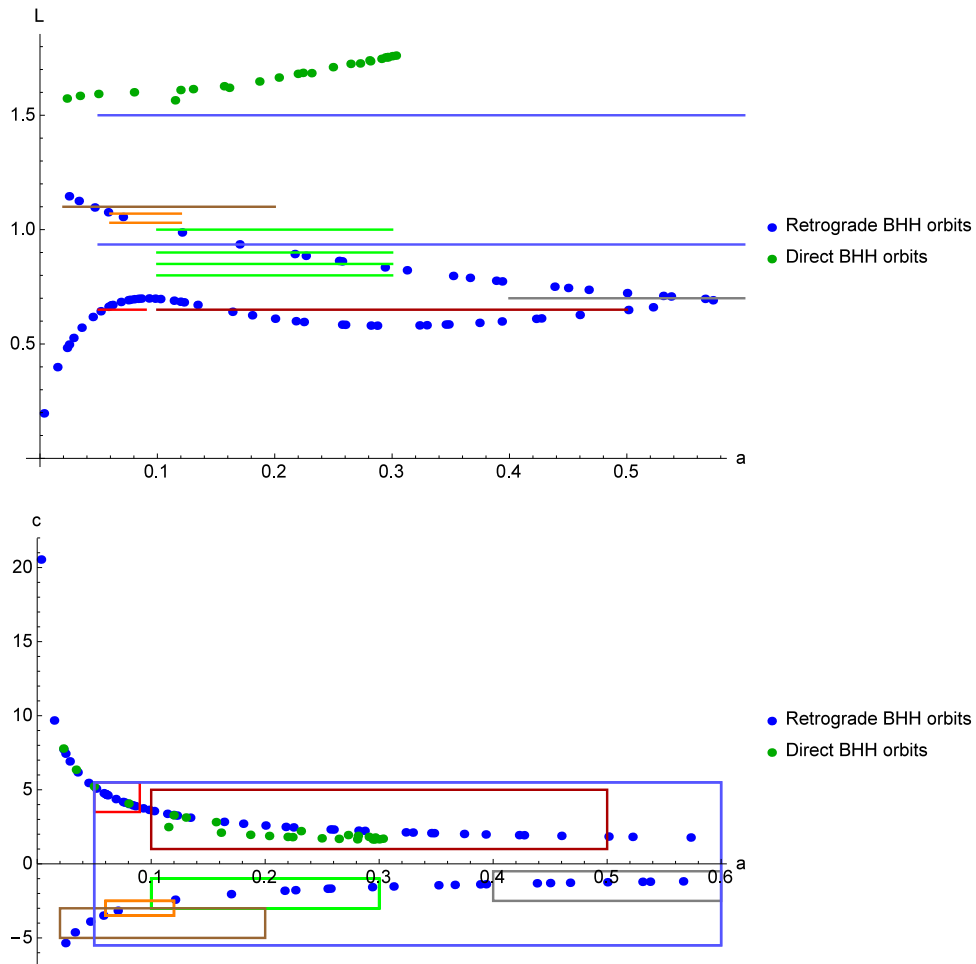
Fig. 9. Illustration of searched segments ("scans") in the parameter spaces (a, L) (upper panel), and (a, c) (lower panel). Each different colored line/box corresponds to a scan we performed in one a–c region, see Table 1, as follows. Upper panel (from top to bottom): blue (1.5)(0.935549), light brown (1.1), orange (1.03)(1.07), green (1.0)(0.9)(0.85)(0.8), gray (0.7), red(0.65), dark brown (0.65). Lower panel: red (0.65), dark brown (0.65), gray (0.7), orange (1.03)(1.07), light brown (1.1), green (0.935549), blue (1.5)(0.935549). (For interpretation of the references to color in this figure legend, the reader is referred to the web version of this article.)

Table 1
Searches ("scans") performed in segments of parameter space.

L	a_{min}	a_{max}	c_{min}	c_{max}	Comment
0.65	0.05	0.09	3.5	5.5	Few local minima
0.65	0.1	0.5	1	5	Several local minima
0.7	0.4	0.6	-2.5	-0.5	Unstructured set of local minima
0.8	0.1	0.3	-3	-1	Good results
0.85	0.1	0.3	-3	-1	Good results
0.9	0.1	0.3	-3	-1	Good results
0.935548917	0.1	0.3	-3	-1	Good results
1	0.1	0.3	-3	-1	Good results
1.03	0.06	0.12	-3.5	-2.5	Good results
1.07	0.06	0.12	-3.5	-2.5	Good results
1.1	0.02	0.2	-5	-3	Many local minima packed densely

5. Kepler-third-law-like regularities

In this section we follow Ref. [39] closely, for two reasons: (1) for the sake of completeness: Kepler-third-law-like regularities are perhaps the most exciting news that have emerged from the discovery of new (satellite) orbits and thus deserve a proper presentation; (2) in order to reveal our methods and way of thinking: we suspect that similar, though perhaps not exactly identical regularities may hold in other families of periodic orbits.

As stated in the Introduction 1, families of periodic three-body orbits can be characterized by the topology of their trajectories in the real configuration space ("braid group"), or on the (so-called) shape sphere ("free group"), as described in Refs. [32–34,51], the latter can be specified by the conjugacy classes of elements, or "words" w, for short, consisting of letters a, b, A = a^{-1}, B = b^{-1}, that define the free group on two letters (a, b).

Thus, here we must study the dependence of the constant on the right-hand-side of the scaling law $T(w)|E(w)|^{3/2} = \text{const}(w)$
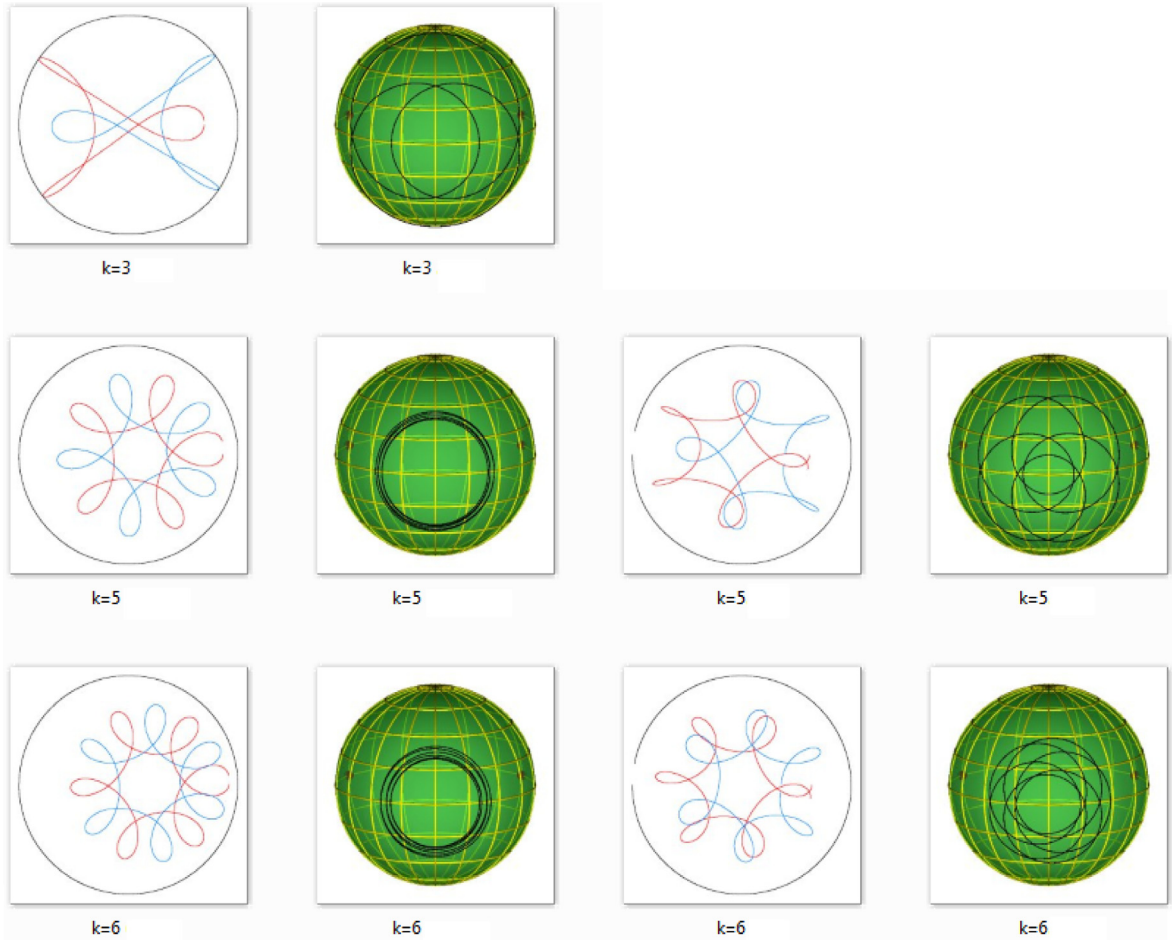
Fig. 10. Examples of satellite orbits of the BHH family, shown in real space and on the shape sphere, $k = 3, 4, 5, 6$. Each row contains two different satellites for each value of $k = 3, 4, 5, 6$, starting from the top, except for $k = 3$, where there is only one.

on the structure of the word $w(a, b, A, B)$ that characterizes a periodic three-body orbit with zero angular-momentum. In Ref. [36] we have shown that Kepler's third law "constant" $T(w^k)|E(w^k)|^{3/2}$ of the "kth satellite orbit" with zero angular-momentum (specified by the free-group element w^k where k is an integer) of the "progenitor orbit" w equals k times the Kepler's third law constant $T(w)|E(w)|^{3/2}$ of the progenitor orbit w: $T(w^k)|E(w^k)|^{3/2} = kT(w)|E(w)|^{3/2}$. More simply, periodic orbits with zero angular-momentum normalized to a common energy E have periods related by $T(w^{k_i}) = k_i T(w)$. We wish to see if this, or some similar statement holds also at non-zero angular momentum?

Then the analogon of Eq. $T(w^k)|E(w^k)|^{3/2} = kT(w)|E(w)|^{3/2}$ for orbits with non-zero angular momenta is

$$T(w^k)|E(w^k)|^{3/2} = f\left(L(w^k)|E(w^k)|^{1/2}\right) = kT(w)|E(w)|^{3/2}$$

$$= kf\left(L(w)|E(w)|^{1/2}\right),$$

or

$$L(w^k)|E(w^k)|^{1/2} = f^{-1}\left(T(w^k)|E(w^k)|^{1/2}\right) = f^{-1}\left(T(w)|E(w)|^{1/2}/k\right)$$

$$= L(w)|E(w)|^{1/2}\left(T(w)|E(w)|^{1/2}/k\right), \quad (7)$$

or yet more simply, a relation between $L(T)$ curves for the progenitor orbit $L_r(T_r)$ and its k'th satellite $L_r^{(w^k)}(T_r^{(w^k)})$:

$$L_r^{(w)}(T_r^{(w)}) = L_r^{(w^k)}(T_r^{(w^k)}/k). \quad (8)$$

In the brief report [39] we tested this relation on the BHH family of solutions using the orbits presented in the previous section. In order to ensure a precise check of Eq. (8) it is necessary to precisely determine orbital periods. The periods T of the orbits could not be reliably established to better than the seven significant digits (decimal places), as shown in Table I in the Supplementary information for Ref. [39].

Our solutions are numerical, hence they necessarily contain some, small, but finite numerical "error", i.e., difference between the particles' spatial positions after one period and their initial values. This error is perhaps best quantified by the value of the "return proximity function", $d(\mathbf{Z}_0, T_0) = \min_{t \leq T_0} |\mathbf{Z}(t) - \mathbf{Z}_0|$, see Refs. [33,34], evaluated after one period $t = T$. The minimal values of $d(\mathbf{Z}_0, T_0)$, $d_{\min}$, for our solutions are typically of the order of $\mathcal{O}(10^{-10}) - \mathcal{O}(10^{-9})$, which also indicates the order of magnitude of the expected error in the values of kinematical variables, such as the period T. The relation between the expected error in the period T and the minimal "return proximity function", $d_{\min}$, is not a linear one, however.

We have undertaken four independent evaluations (denoted by Roman capital numerals I–IV) of period T: two $T(I) = T_{RKF_{rpf}}$, $T(III) = T_{RKF_z}$), are based on the Runge–Kutta–Fehlberg (RKF) algorithm of fourth order, and another two ($T(II) = T_{BS_{rpf}}$, $T(IV) = T_{BS_z}$) are based on the Bulirsch–Stoer (BS) algorithm, each with two different definitions of the period T: T_{rpf} is based on the minimum of the return proximity function (rpf) and T_z is
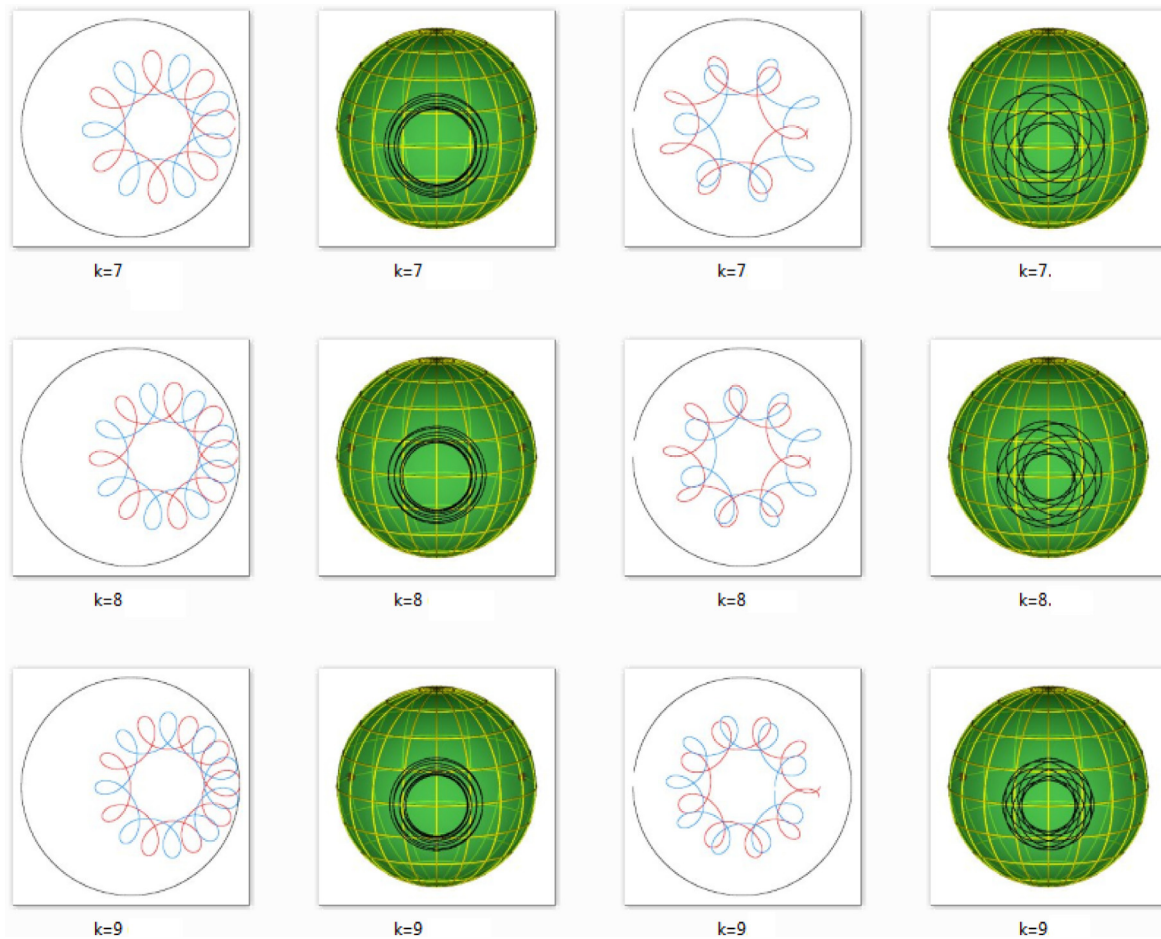
Fig. 11. Examples of satellite orbits of the BHH family, shown in real space and on the shape sphere, $k = 7, 8, 9$. Each row contains two different satellites for each value of $k = 7, 8, 9$, starting from the top.

based on the crossing of the equator on the shape sphere. These measurements may, but need not, agree in general. They must agree only when the initial conditions are "perfect", i.e., when the value of $d(\mathbf{Z}_0, T_0)$ is zero (which does not happen in actual numerical calculations).

5.1. Observed topological dependence of the scaling laws for three bodies

The $L(T)$ curves of different-k satellite orbits are scattered over a large region and do not "touch"/intersect the BHH progenitor family of orbits' $L(T)$ curve when plotted as a function of the (un-divided) period T, see Fig. 13. Note the huge span/scatter of periods in the data.

After dividing the period T by the topological exponent/index k, $T' = T/k$, we can see in Fig. 14 that the satellite orbits' $L(T/k)$ curve (the angular momentum as a function of topologically-rescaled period T/k) approximately coincides with the $L(T)$ curve of BHH retrograde orbits.

6. Open questions

Here we present a list of open questions related to our paper. They range from general questions about astronomical existence and some, perhaps abstract mathematical questions about the deeper underlying causes for these orbits, to entirely practical suggestions as to which specific subspace of i.c.s ought to be explored in a numerical search.

6.1. Astronomical and mathematical questions

Our study also opens up several mathematical and astronomical questions:

1. The BHH family is one of only two families, another being the Lagrange one, of periodic three-body orbits that have been observed in the skies: all "hierarchical" triple star systems belong to BHH orbits, though the converse is not true. The Sun–Earth–Moon system may be viewed as a BHH solution [5,17,20], with unequal masses. Therefore, it seems important to extend the present study to the case of three different masses: some work in this direction has already been done in Refs. [17,20,55], but more needs to be done, and our method lends itself to the task. A number of 3-body systems have been discovered by the *Kepler* space telescope, all of which are of the hierarchical type, see §5.2 and §5.4 in Ref. [5].[17] Are there BHH topological satellites among astronomically observed three-body systems?

2. We have observed satellite orbits only in the stable region of BHH progenitor orbits' $L(T)$ curve: why? What precisely is the relation between satellites' existence and stability of

---

[17] see §5.2 Searches for Exomoons in Ref. [5]: "There are many dynamical processes that affect circumbinary planets, but we will focus on Kepler-16b, the first circumbinary planet confirmed by the Kepler mission (Doyle et al. 2011). This was a huge discovery because previous circumbinary planets had been posited through the post-common envelope binaries (e.g., Beuermann et al. 2010)".
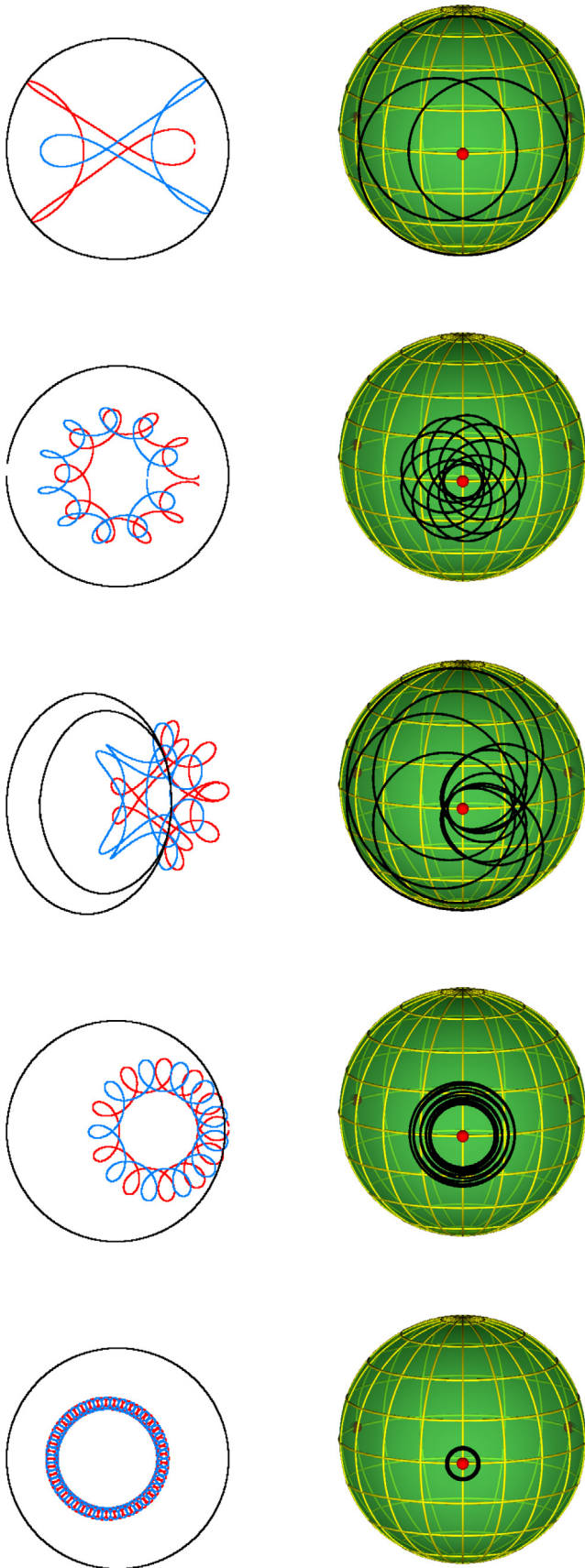
Fig. 12. Overview of some of the satellite orbits in the BHH family, $k = 3, 10, 10, 11, 43$.

progenitor's orbit? In 1976 Hénon [22] stated that "... the stable periodic orbits which we have found are very probably surrounded by a region of finite measure in phase space in which the orbits possess non-linear stability", i.e., that the linearly stable orbits in the BHH three-body family are also nonlinearly, or perpetually, or Kolmogorov–Arnold–Moser (KAM) stable. In other words, the KAM theorem [57–59] is believed to hold for stable BHH orbits. From the KAM theorem it follows that there must be infinitely many "conditionally periodic" solutions near non-linearly stable BHH orbits. In Ref. [37] it was noted that, according to the Birkhoff–Lewis theorem [49], even the (weaker) linear stability may lead to an infinity of periodic satellite orbits. It would be good to verify this conjecture.

3. Prograde orbits are unstable at these values of L, which makes them unlikely to have satellites, according to the Birkhoff–Lewis theorem. One ought to perform further searches in the parameter space at higher values of angular momentum L before one can draw any conclusions about the (non)existence of satellite orbits and their properties on the $L(T)$ plot.

4. In recent years there has been progress in providing formal "proofs of existence" for some BHH orbits, Refs. [26,27]. The obvious question is: can one "prove the existence" of the satellite orbits, and when?

5. Several different types of BHH satellites with identical values of k were reported in Ref. [39]. The question naturally arises: just how many such satellites are there for each value of k?

6. The above point (2) would account for the existence of satellite orbits, though not for the relation between their periods and topologies. Some suggestions about the cause of this relation based on the (complex-variable) analytic properties of the action integral were presented in Appendix E of Ref. [37], but it would be good to make those arguments rigorous, or to repudiate them (for example by finding counterexamples).

6.2. Suggestions for future numerical work

If true, the aforementioned Hénon's conjecture implies existence of infinitely many satellite orbits for all linearly stable three-body orbits, of which there are many. Of course, one may object that a search for all such orbits must be without an end.

However, there is by now sufficient reason to believe that there is some, perhaps not fully revealed as yet, structure in the spectrum of periodic 3-body orbits (*viz.* discrete multiples of periods, relation(s) between periods and topology), and the goal would be to reveal this structure to the fullest extent possible.

Thus, the goal of a search would/ought to be to find (all) linearly stable orbits with the periods shorter than some (finite upper) bound (i.e., with the simplest topologies) — whereas the subsequent extension of sequences (generated by such short orbits — progenitors) towards infinity may indeed be pointless.

6.2.1. Extension of zero-angular-momentum solutions to nonzero values

There are around 20 linearly stable, out of grand total around 200 zero-angular-momentum orbits in Ref. [37] and at least 23 among roughly 2000 orbits from Refs. [35,40,42,43,60].

As explained above, all linearly stable orbits deserve a thorough investigation in the sense of extending them to non-zero angular momenta. Reference [40] commands special attention, because it is the only work that has reported periodic orbits outside of the i.c. subspace defined in Refs. [32,37].
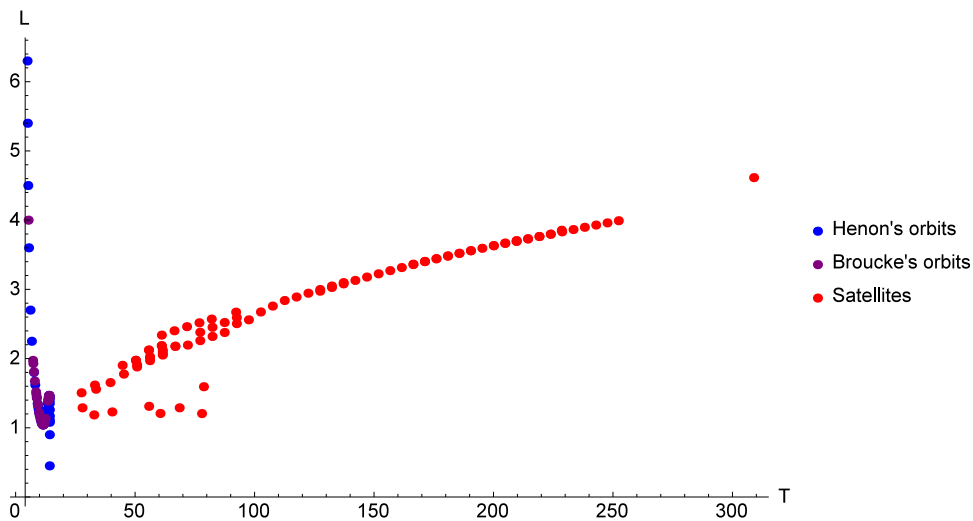
Fig. 13. Retrograde BHH orbits and the BHH satellite orbits with various values of k, discovered thus far, $L(T)$ dependence at fixed energy $E = -0.5$. Adapted from Ref. [39].
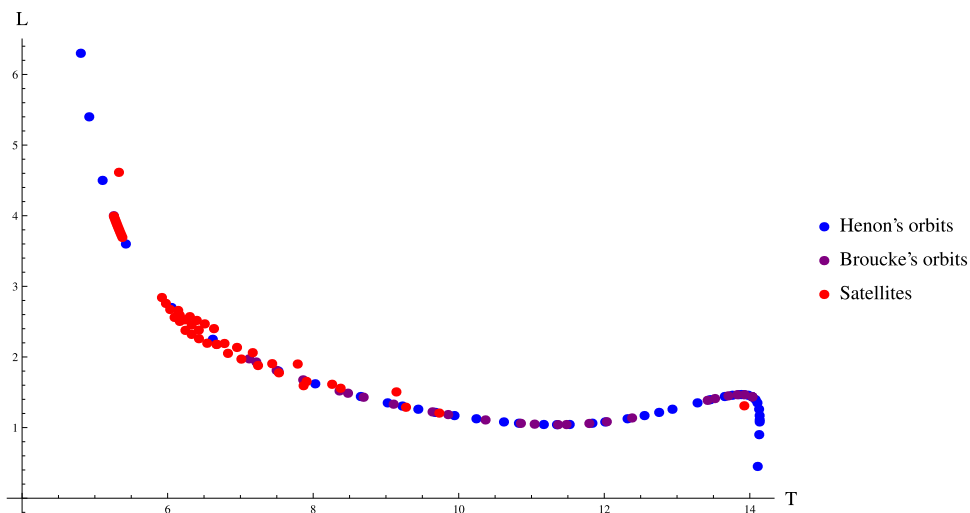
Fig. 14. Retrograde BHH orbits (black and blue dots) and their satellites (red dots) with various values of k, discovered thus far, $L(T' = T/k)$ dependence at fixed energy $E = -0.5$. Adapted from Ref. [39]. (For interpretation of the references to color in this figure legend, the reader is referred to the web version of this article.)

Last, but not least, the same method can be applied to 100, or so, zero angular momentum orbits in the Coulomb potential [50].

6.2.2. Searches around (other) known nonzero-angular-momentum orbits

Of course, search for other satellites can and should be continued in the BHH family, specifically in the prograde orbit branch, where only a few satellites have been found thus far, as well as in the retrograde branch, near the Schubert orbit, where further satellites are expected, but regularization is required [61–63].

There are other known, linearly stable orbits that fall into the present class of initial conditions: Davoust and Broucke reported a number (136) of (generally topologically unidentified) nonzero-angular-momentum orbits in Ref. [44]. All of these orbits' initial conditions are described by four parameters, just as ours, and a number of these orbits are linearly stable. Unfortunately, the

tables of i.c.s in Ref. [44] are (very) difficult to read (due to a bad font) – which prevented us from examining them all[18] – here we discuss only those orbits which we managed to reconstruct.

These orbits were not classified into families according to their topologies, but, rather, using Strömgren's (restricted 3-body problem) classification into 14 *simple symmetry* (denoted by small roman and greek letters) and 11 *double symmetry* families (denoted by capital letters).

Many of these Davoust–Broucke (Strömgren) families fall into one of only three topological families: (1) The (Strömgren) double-symmetry A_1, B and single-symmetry a, b, c, d, α, β families contain orbits with the same topology as the Lagrange–Euler solutions, i.e., the identity element/zero of the free group; (2) The

---

[18] And when we read them, we could not be sure that we did it correctly.

Table 2

The initial conditions in terms of parameters A, B, C, D, as defined in the text, for three semichoreographic orbits. T is the period, L the angular momentum, and E is the energy. The shortest period orbit is Moore's [28].

A	B	C	T	$T|E|^{3/2}$	$L|E|^{1/2}$	E
0.6789245	-1.992169	1.3677159	3.147316	3.6087	-1.7668	-1.0955
0.2369355	-0.720445	1.2540211	8.004531	13.700	0.131881	-1.4308
0.400045	1.415959	1.1166540	8.413701	22.945	6.14072	-1.9519

Table 3

Satellite orbits in the retrograde BHH family, some of which are shown in Fig. 12. Minimal return proximity d_{min} for these orbits is $d_{min} < 10^{-7}$. k is the topological power of the orbit, T is its period and E its energy.

N_r	L	a	c	T	k	d_{min}
1	0.7	0.427052524289	-1.336907801590	4.46125383	3	1.12E$-$10
2	0.85	0.225423376709	-2.161172667330	4.93326124	3	1.72E$-$10
3	0.65	0.226748054608	2.494853501883	5.38634911	3	3.22E$-$11
4	0.85	0.236597473885	-1.986209145030	4.79387855	4	1.09E$-$10
5	0.7	0.410445264670	-0.901755581763	3.04224052	4	1.16E$-$10
6	0.65	0.089473243424	3.863464841380	6.80175586	4	3.88E$-$10
7	0.65	0.351891702719	1.961519344674	5.95736952	4	1.26E$-$10
8	0.8	0.278773932080	-1.610811894950	4.47639401	5	2.26E$-$10
9	0.65	0.131937959644	3.165458555994	8.78754480	5	6.12E$-$08
10	0.8	0.228399714670	-1.771422978980	4.12780456	6	1.12E$-$10
11	0.9	0.162112751455	-2.424555946410	4.72091689	6	1.09E$-$10
12	0.65	0.335276789538	2.040219149776	9.43988995	6	1.38E$-$10
13	0.8	0.195389423297	-1.911145472440	3.90877460	7	2.84E$-$10
14	0.85	0.213186587101	-1.831539642360	4.45339868	7	1.61E$-$10
15	0.9	0.174854596011	-2.217240443720	4.74829390	7	9.79E$-$11
16	0.9	0.269439116363	-1.452760161970	4.74215052	7	1.87E$-$10
17	0.8	0.171971993864	-2.034163513840	3.75598535	8	1.38E$-$10
18	0.935548917	0.129471314426	-2.721144023250	4.76584900	8	1.01E$-$10
19	0.7	0.537026752182	-1.208756213130	15.23729361	8	1.49E$-$10
20	0.85	0.186299773074	-1.955937487530	4.23559872	8	1.45E$-$10
21	0.9	0.205445523859	-1.864664426590	4.90547644	8	1.26E$-$10
22	0.935548917	0.273518188668	-1.304218790410	4.75908509	8	1.34E$-$10
23	0.8	0.154250567982	-2.146266402400	3.64212942	9	3.05E$-$10
24	0.935548917	0.232402133831	-1.514749892810	4.78046677	9	9.95E$-$11
25	0.85	0.166323483739	-2.067914324720	4.07742799	9	2.21E$-$10

(Strömgren) double-symmetry family A_2 contains quasi-isosceles orbits (with angular momentum); (3) The (Strömgren) double-symmetry families D_1, E, G and single-symmetry g, h, i are (direct) parts of the BHH topological family; (4) The (Strömgren) double-symmetry D_2, D_3, D_4, F and single-symmetry e families are (retrograde) parts of the BHH topological family, in particular solutions no. 90 and no. 91 are the $k = 3$ satellites.

6.2.3. Semichoreographies with nonzero-angular-momentum

Davoust and Broucke [44] were apparently the first ones to find a semichoregraphic solution — a periodic 3-body orbit wherein two bodies move on the same trajectory, whereas the third one moves on its own. In Ref. [28] Moore rediscovered Davoust and Broucke's orbit. We have found two other such orbits, see Table 2, and called them semichoreographies; each (semi)choreography defines a continuous family of orbits, as a function of angular momentum, whose orbits are not (necessarily) semichoreographies themselves, and which have not been explored thus far, to our knowledge.

We list several such orbits' i.c.s in Table 2, with the following definition of i.c. parameters A, B, C, D in terms of our parameters a, b, c, d,

$$a = \sqrt{2}, \quad b = -\sqrt{\frac{2}{3}}A, \quad c = \sqrt{\frac{1}{2}}(B - C), \quad d = \sqrt{\frac{3}{2}}(B + C).$$

6.2.4. Isolated orbits

Last, but not least there are a number of isolated, generally topologically unidentified periodic orbits, often unpublished, or published only in Ph.D. or M.Sc. theses, and/or on the internet; here we list the ones we knew at the time of writing.

- The "Celtic knot" choreographic orbit of Montaldi & Steckles [64] (no i.c.s supplied), which appears to be equivalent to the "Rosette" orbit of Grant [56] with nonvanishing angular momentum, the i.c.s are supplied in footnote [91]. This orbit does not fit into the (sub)space of collinear orthogonal i.c.s, for proof, see footnote,[19] and therefore requires relaxation of conditions imposed in Section 3.2.
- Danya Rose's many previously unknown orbits with vanishing angular momentum [40], some of which do not pass through an equidistant collinear ("Eulerian") initial configuration.
- A number of as yet topologically unidentified orbits presented in Refs. [55,65] and references therein.

All of this indicates: (1) a need to complete the families with other non-zero angular momentum orbits; (2) a probable abundance of new satellite orbits waiting to be discovered.

Free-fall orbits generally do not satisfy $\dot{R} = 0$ at equator crossings,[20] so generally they do not fall into the present search space.

---

[19] In order to check if its i.c.s fall into the class of collinear orthogonal, i.e., if $\mathbf{r}_i \cdot \dot{\mathbf{r}}_i = 0$, (for all $i = 1, 2, 3$), we note that the first of six syzygies is reached after $t = 0.7032783$, where we have $(x_1(t), y_1(t), x_2(t), y_2(t), x_3(t), y_3(t)) = (0.00077832, -0.469023, -0.00165945, 0.999997, 0.000881126, -0.530975)$, which still has 4 independent variables. Of course, two of these four can be eliminated by an appropriate rotation of the reference frame. Similarly, the velocities at $t = 0.7032783$ are $(\dot{x}_1(t), \dot{y}_1(t)) = (-3.03236, -2.77587)$; $(\dot{x}_2(t), \dot{y}_2(t)) = (0.385354, 0.00774803)$; $(\dot{x}_3(t), \dot{y}_3(t)) = (2.647, 2.76812)$, of which there are 4 independent ones. Evaluating the scalar products, which are rotation-invariant, we see that $\mathbf{r}_i \cdot \dot{\mathbf{r}}_i \neq 0$ (for all $i = 1, 2, 3$), i.e., this is not an orthogonal collinear configuration. Nevertheless, this orbit passes through three reversible configurations of another kind: the isosceles one, see Ref. [65].

[20] With the exception of isosceles triangle ones.

Table 4
Satellite orbits in the retrograde BHH family — Table 3 continued.

N_r	L	a	c	T	k	d_{min}
26	0.9	0.182069791972	−1.978004135720	4.67040604	9	1.17E−10
27	0.935548917	0.137285145946	−2.545654735050	4.78370980	9	9.67E−11
28	1	0.294303286736	−1.008322699800	4.76801186	9	1.23E−10
29	1	0.238218402625	−1.735467337160	6.99274465	9	1.40E−10
30	0.85	0.150808938415	−2.170190077810	3.95629338	10	1.48E−10
31	1	0.209243455808	−1.847936324290	6.46969425	10	1.57E−10
32	1	0.266925744815	−1.097311225480	4.78597293	10	1.23E−10
33	0.7	0.442402892100	−0.700265953090	6.66684025	10	2.26E−09
34	0.8	0.129160165070	−2.343250256240	3.48168164	11	1.12E−10
35	1	0.243617171755	−1.190238664360	4.79985962	11	1.09E−10
36	0.8	0.119882517495	−2.431498122390	3.42239489	12	1.27E−10
37	0.935548917	0.147716034231	−2.192473293620	4.68169607	12	1.18E−10
38	1	0.223340706817	−1.288029535680	4.81093626	12	2.30E−10
39	0.8	0.112051269923	−2.514553762900	3.37232423	13	1.43E−10
40	0.935548917	0.137088743692	−2.274985930540	4.56392294	13	1.52E−10
41	1	0.205347639306	−1.392000632830	4.81998871	13	1.62E−10
42	0.8	0.105352054293	−2.592836811550	3.32933694	14	1.97E−10
43	1	0.146284147722	−2.203021298400	5.44909516	14	1.06E−10
44	0.85	0.105854763654	−2.586702862280	3.60999927	15	1.05E−10
45	1	0.136829854037	−2.277089258430	5.30678948	15	2.09E−10
46	1	0.173982588477	−1.627461935580	4.83391624	15	5.74E−09
47	0.85	0.100315012262	−2.656853706660	3.56736722	16	9.88E−11
48	0.9	0.102148274757	−2.632996062570	3.90923742	17	1.52E−10
49	0.935548917	0.102773178918	−2.625007735230	4.19114405	18	1.04E−10
50	1	0.110009104810	−2.537603649510	4.91429079	19	1.42E−08

7. Summary, conclusions

Here we have presented details of our method, originally designed to search for periodic orbits within the Broucke–Hadjidemetriou–Hénon (BHH), Refs. [17–23], family of orbits. However, we have realized that the method has a (much) wider scope.

We have numerically found 99 new satellite orbits in the family of BHH relative periodic solutions to the planar three body problem, and analyzed their properties and compared them with the properties of the original BHH orbits. An approximate relation between their kinematic and topological properties was reported in Ref. [39].

BHH orbits form a family with a very simple topology, and their satellites are orbits with topology that can be described as the kth power of BHH one. The BHH orbits' scale-invariant angular momenta L and scale-invariant periods T form a continuous curve $L(T)$, whereas our satellite orbits form a scattered set of points on the same $L(T)$ plot. The latter exhibit the property that when their period T is divided by their "topological power" k, they approximately fall on the $L(T)$ curve of the original ($k = 1$) BHH orbits. The deviation from exact identity of the two curves, can be quantified by a mean-square-root deviation of the observed satellite-orbit data from a fit to the BHH progenitor-orbit data.

Our study was motivated by the discovery of satellite orbits at vanishing angular momentum and of the proportionality of their scale-invariant period to their topological power [33]. The Kepler-like topological regularities have been found to hold more generally in sequences of orbits, albeit thus far only at vanishing angular momenta [36,37]. This report shows, however, that this regularity persists even when orbits with $L \neq 0$ are considered, albeit approximately, i.e., within some tolerance.

These results are even more striking when one remembers that there are several distinct types of satellite orbits of the same topological power k, some with quite different values of L and T, all of which display this property. Furthermore, more than one satellite of the same power k and the same type have been found for several progenitor orbits presented in this report; our results (not shown here) suggest that satellites form continuous

Table 5
Satellite orbits in the retrograde BHH family — Tables 3 and 4 continued.

N_r	L	a	c	T	k	d_{min}
51	1.03	0.111843109779	−2.516815645433	5.31721934	20	9.76E−11
52	1.03	0.106999360702	−2.572864154118	5.23675314	21	1.10E−10
53	1.03	0.102629340641	−2.626824252565	5.16461551	22	1.04E−10
54	1.07	0.112532299117	−2.509130097108	5.93058960	22	9.37E−11
55	1.03	0.098663558847	−2.678884782752	5.09949046	23	1.13E−10
56	1.07	0.107950445783	−2.561552366744	5.83679015	23	1.62E−10
57	1.03	0.095045815614	−2.729207988143	5.04033295	24	1.24E−10
58	1.07	0.103792166702	−2.612125153377	5.75238033	24	9.83E−10
59	1.07	0.099998313989	−2.661009860717	5.67592271	25	1.93E−10
60	1.07	0.096520577947	−2.708345753387	5.60626742	26	1.77E−10
61	1.07	0.093319072567	−2.754253774713	5.54248254	27	1.28E−10
62	1.07	0.090360532835	−2.798839977984	5.48380387	28	1.27E−10
63	1.07	0.087616970029	−2.842197991476	5.42959820	29	1.09E−10
64	1.03	0.078546062730	−3.001449136918	4.77275161	30	1.18E−10
65	1.07	0.085064647578	−2.884410942736	5.37933595	30	1.04E−10
66	1.03	0.076424987284	−3.042734364817	4.73851381	31	1.48E−10
67	1.07	0.082683286816	−2.925553119986	5.33257043	31	1.02E−10
68	1.03	0.074436173120	−3.083042211579	4.70642108	32	1.04E−10
69	1.07	0.080455449983	−2.965691193228	5.28892198	32	9.96E−11
70	1.03	0.072567055606	−3.122428961620	4.67626201	33	1.51E−10
71	1.07	0.078366051119	−3.004885281315	5.24806564	33	1.39E−10
72	1.03	0.070806647363	−3.160945841855	4.64785297	34	9.95E−11
73	1.07	0.076401964229	−3.043189884203	5.20972146	34	1.05E−10
74	1.03	0.069145295338	−3.198639607087	4.62103356	35	1.66E−10
75	1.07	0.074551712461	−3.080654510153	5.17364685	35	1.59E−10

curves in the parameter space of initial conditions. That "fine structure" should be investigated in greater detail, however, as in the examples set by Davoust and Broucke [44].

From the methodological point of view, we have shown that a systematic search for periodic solutions is possible in a three-dimensional subspace of initial conditions, although it is more challenging and time-consuming than in the case of orbits with vanishing angular momentum. We have found satellite orbits up to topological power $k = 58$ (84); but we feel that we have not found all satellite orbits with values $k \leq 58$ (84), despite there being no known theorem stating how many orbits there ought to be. It should be noted that our search was time-limited: the same method can be used without modifications to complete the

Table 6
Satellite orbits in the retrograde BHH family — Tables 3–5 continued.

N_r	L	a	c	T	k	d_{min}
76	1.03	0.067574480868	−3.235553106562	4.59566306	36	1.02E−10
77	1.03	0.066086655842	−3.271725713345	4.57161742	37	1.18E−10
78	1.07	0.071153562285	−3.153240705933	5.10748717	37	1.01E−10
79	1.03	0.064675107247	−3.307193655949	4.54878679	38	1.05E−10
80	1.07	0.069588876352	−3.188441664622	5.07705416	38	1.04E−10
81	1.1	0.072454170036	−3.124853635110	5.53965642	39	1.05E−10
82	1.03	0.063333841711	−3.341990448546	4.52707358	39	1.68E−10
83	1.07	0.068104140192	−3.222962078095	5.04818753	39	1.04E−10
84	1.1	0.070912224143	−3.158592700200	5.50480009	40	9.94E−11
85	1.03	0.062057492484	−3.376147044334	4.50639068	40	1.13E−10
86	1.1	0.069446525539	−3.191702128170	5.47170776	41	1.07E−10
87	1.03	0.060841236077	−3.409692239688	4.48666015	41	1.03E−10
88	1.07	0.065350113732	−3.290088012685	4.99465663	41	9.97E−11
89	1.07	0.065350112192	−3.290088080655	4.99465659	41	1.15E−10
90	1.1	0.068051285222	−3.224210823950	5.44023825	42	1.04E−10
91	1.03	0.059680728422	−3.442652640917	4.46781196	42	1.24E−10
92	1.1	0.066721298871	−3.256145631480	5.41026552	43	8.88E−11
93	1.07	0.069589283429	−2.997571148119	4.88748351	43	1.26E−10
94	1.1	0.065451870057	−3.287531720240	5.38167667	44	1.02E−10
95	1.1	0.064238759898	−3.318392179570	5.35437026	45	1.03E−10
96	1.1	0.063078117801	−3.348748949910	5.32825481	46	2.14E−10
97	1.1	0.061966455334	−3.378621962290	5.30324770	47	9.76E−11
98	1.1	0.060900580973	−3.408030582910	5.27927394	48	9.86E−11
99	0.93555	0.061515814146	1.086851979730	2.57459301	58	1.96E−10

search. We concentrated on a search for satellites of retrograde BHH orbits, yet in this process we inadvertently found (only) four satellites of direct BHH orbits.

There is no reason to believe, however, that a finite maximum value of k exists. As k increases the satellite orbits seem to be packed more densely, however, so the search for higher values of k will be limited by inevitable numerical inaccuracies.

Our method can be also used without modification to extend this search to higher angular momenta and to direct BHH orbits. An extension of our search into unexplored regions of the $L - T$ plane ought to provide (new) data that will further test our hypothesis.

Last, but not least, the same method can be used to search for non-vanishing angular momentum families of orbits other than the BHH one, as explained in Section 6.2. That, of course, would represent a major new research program.

Declaration of competing interest

The authors declare that they have no known competing financial interests or personal relationships that could have appeared to influence the work reported in this paper.

Acknowledgments

Appendix A. Tables of initial conditions

For the sake of reproducibility, here we list the initial conditions of our 99 orbits.

A.1. Arbitrary k satellites

Tables 3, 4, 5, 6 show initial conditions for un-normalized orbits.

References

[1] C. Marchal, The Three-Body Problem, Elsevier Science Publishers, Amsterdam, 1990.
[2] Mauri Valtonen, Joanna Anosova, Konstantin Kholshevnikov, Aleksandr Mylläri, Victor Orlov, Kiyotaka Tanikawa, The Three-Body Problem from Pythagoras To Hawking, Springer International Publishing, Switzerland, 2016.
[3] M. Valtonen, H. Karttunen, The Three-Body Problem, Cambridge University Press, 2005.
[4] Kenneth R. Meyer, Glen R. Hall, Dan Offin, Introduction To Hamiltonian Dynamical Systems and the N-Body Problem, second ed., Springer, New York, 2009.
[5] Zdzislaw Musielak, Billy Quarles, Three Body Dynamics and Its Applications To Exoplanets, in: SpringerBriefs in Astronomy, 2017.
[6] L. Euler, Nov. Comm. Acad. Imp. Petropolitanae 10 (1740) 207–242; L. Euler, Nov. Comm. Acad. Imp. Petropolitanae 11 (1740) 152–184; Mémoires de l'Acad. de Berlin 11 228–249.
[7] J.L. Lagrange, Oeuvres tome 6; Miscellanea Taurinensia 4 (1772) 118–243; Oeuvres 2 67–121; Mécanique Analytique 262–286; second ed., vol. 2, pp. 108–121; Oeuvres 12 101–114.
[8] A. Tokovinin, in: N. St-Louis, A.F.J. Moffat (Eds.), Massive Stars in Interacting Binaries, in: ASP Conference Series, vol. 367, 2007, pp. 615–619.
[9] J. Schubart, Astron. Nachr. 283 (1956) 17.
[10] R. Vernić, Hrvatsko Prirod, Društvo Clas. Mat. Fiz. Astron. Ser. 2 8 (1953) 247–266.
[11] R.F. Arenstorf, in: J.K. Hale, J.P. Lasalle (Eds.), Differential Equations and Dynamical Problems, Academic Press, 1967, pp. 55–68.
[12] W.H. Jefferys, J. Moser, Astron. J. 71 (1966) 568–578.
[13] V. Szebehely, C.F. Peters, Astron. J. 72 (1967) 876–883.
[14] V. Szebehely, C.F. Peters, Astron. J. 72 (1967) 1187–1190.
[15] E.M. Standish, in: G.E.O. Giacaglia (Ed.), Periodic Orbits, Stability and Resonances, D. Reidel Publ. Co., Dordrecht, Holland, 1970, pp. 375–381.
[16] M. Hénon, Celest. Mech. 10 (1974) 375.
[17] R. Broucke, D. Boggs, Celest. Mech. 11 (1975) 13.
[18] R. Broucke, Celest. Mech. 12 (1975) 439.
[19] J.D. Hadjidemetriou, Celest. Mech. 12 (1975) 155.
[20] J.D. Hadjidemetriou, Th. Christides, Celest. Mech. 12 (1975) 175.
[21] J.D. Hadjidemetriou, Celest. Mech. 12 (1975) 255.

[22] M. Hénon, Celest. Mech. 13 (1976) 267.
[23] M. Hénon, Celest. Mech. 15 (1977) 243.
[24] M. Hénon, Celest. Mech. 15 (1977) 99.
[25] L.D. Landau, E.M. Lifshitz, Mechanics, third ed., Butterworth-Heinemann, Oxford, 1976.
[26] Kuo-Chang Chen, Ann. of Math. 167 (2008) 325–348.
[27] Kuo-Chang Chen, Yu-Chu Lin, Commun. Math. Phys. 291 (2009) 403–441.
[28] C. Moore, Phys. Rev. Lett. 70 (1993) 3675.
[29] A. Chenciner, R. Montgomery, Ann. of Math. 152 (2000) 881–901.
[30] C. Simó, in: Alain Chenciner, Richard Cushman, Clark Robinson, Zhihong Jeff Xia (Eds.), Celestial Mechanics, in: Contemporary Mathematics, vol. 292, AMS, Providence, R.I, 2002, p. 209.
[31] A.I. Martynova, V.V. Orlov, A.V. Rubinov, Astron. Rep. 53 (2009) 710.
[32] M. Šuvakov, V. Dmitrašinović, Phys. Rev. Lett. 110 (2013) 114301.
[33] Milovan Šuvakov, Celestial Mech. Dynam. Astronom. 119 (2014) 369–377.
[34] M. Šuvakov, V. Dmitrašinović, Amer. J. Phys. 82 (2014) 609–619.
[35] P.P. Iasko, V.V. Orlov, Astron. Rep. 58 (11) (2014) 869–879.
[36] V. Dmitrašinović, M. Šuvakov, Phys. Lett. A 379 (2015) 1939–1945.
[37] V. Dmitrašinović, Ana Hudomal, Mitsuru Shibayama, Ayumu Sugita, J. Phys. A 51 (2018) 315101, physics.
[38] http://three-body.ipb.ac.rs/ and http://three-body.ipb.ac.rs/sequences.php.
[39] M.R. Janković, V. Dmitrašinović, Phys. Rev. Lett. 116 (5) (2016) 064301.
[40] Danya Rose, Geometric Phase and Periodic Orbits of the Equal-Mass, Planar Three-Body Problem with Vanishing Angular Momentum (Ph.D. thesis), University of Sydney, 2016, Available at https://ses.library.usyd.edu.au/h{and}le/2123/14416.
[41] Milovan Šuvakov, Mitsuru Shibayama, Celestial Mech. Dynam. Astronom. 124 (2016) 155–162.
[42] X. Li, Y. Jing, S. Liao, Publ. Astron. Soc. Japan 057 (2018) 1–7.

[43] Xiaoming Li, Shijun Liao, Sci. China A 60 (12) (2017) 129511.
[44] E. Davoust, R. Broucke, Astron. Astrophys. 112 (1982) 305–320.
[45] M. Nauenberg, Phys. Lett. A 292 (2001) 93–99.
[46] M. Nauenberg, Celest. Mech. 97 (2007) 1.
[47] A. Chenciner, J. Fejoz, R. Montgomery, Nonlinearity 18 (2005) 1407–1424.
[48] R. Broucke, A. Elipe, A. Riaguas, Chaos Solitons Fractals 30 (2006) 513–520.
[49] G.D. Birkhoff, D.C. Lewis, Ann. Mat. 12 (4) (1933) 117–133.
[50] M. Šindik, A. Sugita, M. Šuvakov, V. Dmitrašinović, Phys. Rev. E 98 (2018) 060101.
[51] R. Montgomery, Nonlinearity 11 (1998) 363–376.
[52] R. Montgomery, Ergodic Theory Dynam. Systems 27 (6) (2007) 1933–1946.
[53] A.E. Roy, M.W. Ovenden, Mon. Not R. Astron. Soc. 115 (1955) 296–309.
[54] A. Vanderbauwhede, Discrete Contin. Dyn. Syst. Ser. A 33 (2013) 359.
[55] Abimael Bengochea, Jorge Galán, Ernesto Pérez-Chavela, Astrophys. Space Sci. 348 (2013) 399–415.
[56] Martin Eric Grant, of Las Positas College 3000 Campus Hill Drive Livermore CA 94551, private communication, Jan 8, 2018, <martin@ramblemuse.com>. See also https://math.stackexchange.com/questions/1851339/possibly-new-solution-to-equal-mass-three-body-problem-refinement-required.
[57] A.N. Kolmogorov, Dokl. Akad. Nauk. SSSR 98 (1954) 527–530 (in Russian).
[58] V.I. Arnold, A.N. Proof of, Russian Math. Surveys 18 (1963) 9–36.
[59] J. Moser, Nachr. Akad. Wiss. Göttingen Math. Phys. Kl. IIa 1 (1962) 1–20.
[60] P.P. Iasko, V.V. Orlov, Astron. Rep. 59 (5) (2015) 404–413.
[61] T. Levi-Civita, Acta Math. 30 (1906) 305–327, Opere Matematiche, vol. 2, Bologna, 1956, p. 419.
[62] T. Levi-Civita, Acta Math. 42 (1920) 99–144.
[63] P. Kustaanheimo, E.L. Stiefel, Reine Angew. Math. 218 (1965) 204.
[64] James Montaldi, Katrina Steckles, Classification of symmetry groups for planar n-body choreographie, arXiv:1305.0470, see also: http://www.maths.manchester.ac.uk/jm/Choreographies/.
[65] Abimael Bengochea, Jorge Galán, Manuel Falconi, Astrophys. Space Sci. 333 (2011) 40–408.